


ORIGINAL RESEARCH

Silicon ameliorates clubroot responses in canola (*Brassica napus*): A “multi-omics”-based investigation into possible mechanisms

Ananya Sarkar¹ | Anna Kisiala² | Dinesh Adhikary¹ | Urmila Basu¹ |
R. J. Neil Emery² | Habibur Rahman¹ | Nat N. V. Kav¹ 

¹Department of Agricultural, Food & Nutritional Science, University of Alberta, Edmonton, Alberta, Canada

²Biology Department, Trent University, Peterborough, Ontario, Canada

Correspondence

Nat N. V. Kav, Department of Agricultural, Food & Nutritional Science, University of Alberta, Edmonton, AB, Canada.
Email: nat@ualberta.ca

Funding information

Results Driven Agricultural Research (RDAR), Grant/Award Number: #2020F004R

Edited by R.M. Rivero

Abstract

Clubroot disease, caused by *Plasmodiophora brassicae* Woronin, results in severe yield losses in Brassica crops, including canola. Silicon (Si) mitigates several stresses and enhances plant resistance to phytopathogens. We investigated the effects of Si on clubroot disease symptoms in canola at two concentrations of Si, Si: soil in 1:100 w/w (Si1.0) and Si: soil in 1:200 w/w (Si0.5) under greenhouse conditions. In addition, the effects of Si on *P. brassicae*-induced gene expression, endogenous levels of phytohormones and metabolites were studied using “omics” approaches. Si application reduced clubroot symptoms and improved plant growth parameters. Gene expression analysis revealed increased transcript-level responses in Si1.0 compared to Si0.5 plants at 7-, 14-, and 21-days post-inoculation (dpi). Pathogen-induced transcript-level changes were affected by Si treatment, with genes related to antioxidant activity (e.g., *POD*, *CAT*), phytohormone biosynthesis and signalling (e.g., *PDF1.2*, *NPR1*, *JAZ*, *IPT*, *TAA*), nitrogen metabolism (e.g., *NRT*, *AAT*), and secondary metabolism (e.g., *PAL*, *BCAT4*) exhibiting differential expression. Endogenous levels of phytohormones (e.g., auxin, cytokinin), a majority of the amino acids and secondary metabolites (e.g., glucosinolates) were increased at 7 dpi, followed by a decrease at 14- and 21-dpi due to Si-treatment. Stress hormones such as abscisic acid (ABA), salicylic acid (SA), and jasmonic acid (JA) also decreased at the later time points in Si0.5, and Si1.0 treated plants. Si appears to improve clubroot symptoms while enhancing plant growth and associated metabolic processes, including nitrogen metabolism and secondary metabolite biosynthesis.

1 | INTRODUCTION

Canola (*Brassica napus* L.) is an economically important oilseed crop, with 70.62 million metric tons (MMT) produced globally in 2021–2022 (Statista, 2022). It is a healthy oil due to its low content of

saturated (7%), high contents of monounsaturated (62%), and polyunsaturated (32%) fatty acids (Lin et al., 2013). Canola production is, however, threatened by several biotic stresses, among which the clubroot disease caused by the soil-borne obligate pathogen *Plasmodiophora brassicae* (Woronin, 1878) is the most important. This disease

This is an open access article under the terms of the [Creative Commons Attribution-NonCommercial-NoDerivs](https://creativecommons.org/licenses/by-nc-nd/4.0/) License, which permits use and distribution in any medium, provided the original work is properly cited, the use is non-commercial and no modifications or adaptations are made.

© 2023 The Authors. *Physiologia Plantarum* published by John Wiley & Sons Ltd on behalf of Scandinavian Plant Physiology Society.

results in “club”-shaped roots, which restricts the transportation of water and nutrients to the shoots and results in significant crop losses (Kageyama & Asano, 2009). Clubroot disease affects cruciferous crops in more than 60 countries resulting in 10–15% yield loss globally (Dixon, 2009a).

P. brassicae is a biotrophic protist under the phylum Plasmodiophoromycota (Barr, 1992), and it can survive in infested fields as resting spores for over 17 years (Wallenhammar, 1996). These resting spores infect root hairs and epidermal cells at the root differentiation zone, initiating primary infection (Liu et al., 2020). The secondary infection occurs in the root cortex resulting in cellular hypertrophy and visible gall formation in the susceptible hosts (Kageyama & Asano, 2009; Liu et al., 2020). The use of clubroot-resistant (CR) cultivars is considered an environmental-friendly strategy for controlling this disease (Rahman et al., 2014). However, growing the same CR cultivar for a few years can impose selection pressure on *P. brassicae* populations resulting in the evolution of novel pathotypes (Strelkov et al., 2016). To date, 36 pathotypes have been identified in Canada, of which 19 can overcome the resistance of the “first generation” CR cultivars (Askarian et al., 2021; Hollman et al., 2021).

P. brassicae is a soil-borne pathogen; therefore, the chemical and physical conditions of the soil influence clubroot disease incidence; for instance, acidic soils favour the germination of resting spores (Dixon, 2009b). Therefore, soil amendments with calcium compounds are used to neutralize the pH, which reduces disease severity (Fox et al., 2022). Using bait crops (Ahmed et al., 2011), and rotation with cereal and legume crops for more than 2 years can also reduce the soil spore concentrations by ~90% (Peng et al., 2015). However, the lack of adequate management practices and the evolution of novel pathotypes warrant additional research to mitigate this problem using other approaches.

Silicon (Si) is the second most abundant element on earth (after oxygen), accounting for 28.8% of the mass of the earth's crust. Plant roots take up Si in the form of soluble monosilicic acid ($\text{Si}(\text{OH})_4$) and translocate it via the xylem to the above-ground parts, where they are deposited as silica (SiO_2) (Epstein, 2009). Si accumulation in plants varies between 0.1% and 10% by dry weight, and cellular accumulation occurs through the plasma membrane via the Lsi1 (Low silicon 1) and Lsi2 (Low silicon 2) transporters, belonging to nodulin-26-like major intrinsic protein family (NIPs) and anion transporter family, respectively (Ma et al., 2006, 2007). Si is mainly found as soil mineral silicates, some soluble Si sources include wollastonite and slag, and can be applied as a soil-based fertilizer or foliar spray to improve crop productivity (Zellner et al., 2021).

Si application in the presence of phytopathogens was initially thought to result in the formation of a physical barrier by the deposition of phytoliths (SiO_2), thereby reducing pathogen infection (Kim et al., 2002). Subsequently, several studies revealed that Si application induces local and systemic defence responses through elevated defence-related enzymes (e.g., peroxidases), secondary metabolites/phytoalexins as well as salicylic acid (SA) and jasmonic acid (JA)-mediated systemic signalling (Fauteux et al., 2005, 2006). Rasoolizadeh

et al. (2018) reported that Si treatment increased resistance to *Phytophthora sojae* in soybean through an incompatible host-pathogen reaction, leading to reduced pathogen effector gene expression. Si application has been reported to mitigate biotic stress in several crops against a wide range of pathogens (reviewed in Wang et al., 2017, and references therein).

Omics approaches have provided a molecular-level understanding of plant-pathogen interactions and widened the prospects for improving clubroot resistance in canola. Using these approaches, the differential expression of genes, including those involved in the activation of reactive oxygen species (ROS), SA- and JA- mediated signalling, sugar transport, cell-wall modifications and phenylpropanoid biosynthesis have been reported (Adhikary, Kisiala, et al., 2022a; Galindo-González et al., 2020; Summanwar et al., 2021). In addition, metabolomics-based approaches have implicated the involvement of metabolites like citric acid and glucosinolates (Wagner et al., 2019), as well as the phytohormone SA (Lan et al., 2020) in mediating resistance to clubroot. Multi-omics-based approaches involving transcriptomics and metabolomics have revealed altered metabolites as well as their associated transcripts in response to clubroot in *B. napus* (Adhikary, Kisiala, et al., 2022a; Aigu et al., 2022). Therefore, multiple omics approaches have significant potential in investigating molecular changes that accompany clubroot disease resistance.

In this study, we evaluated the potential role of Si in reducing clubroot disease in canola under greenhouse conditions. We characterized the *P. brassicae*-mediated changes in gene expression, phytohormones, and metabolites in the presence or absence of Si. This is the first report on the effects of Si on clubroot disease progression in canola as well as Si-induced changes in gene expression, phytohormone and metabolite profiles.

2 | MATERIALS AND METHODS

2.1 | Soil amendment with silicon and experimental setup

Sodium silicate (Na_2SiO_3 , Sigma-Aldrich) was mixed with 100 g Sunshine Professional Growing Mix (Sun Gro Horticulture), and the following mixtures (treatments) were produced: 0.0 g Si (control, PC), 0.1 g Si (Si: soil in 1:1000, w/w), 0.25 g (Si: soil in 1:400, w/w), 0.5 g (Si: soil in 1:200, w/w), 0.75 g (Si: soil in 3:400, w/w), and 1.0 g (Si: soil in 1:100, w/w). Hereafter, these treatments are reported as PC, Si0.1, Si0.25, Si0.5, Si0.75, and Si1.0, respectively. After mixing thoroughly, the pH of the soil mix was determined prior to seeding. A clubroot susceptible spring canola (*Brassica napus* L.) cultivar Hi-Q, developed at the University of Alberta, was used in this study. The plants were grown under greenhouse conditions (22/19°C and 16/8 h photoperiod, 30% relative humidity) on soil mixtures containing varying concentrations of Si. A total of 30 plants from three replications of each treatment (i.e., 10 plants per replication) were used.

2.2 | Pathogen inoculation, assessment of disease severity, and histology

A single spore suspension of *P. brassicae* pathotype 3, classified as pathotype 3H (P3H) under the Canadian Clubroot Differential (CCD) set (Strelkov et al., 2018), was prepared by homogenizing the clubroot galls. The spore concentration was adjusted to 10^7 CFU mL⁻¹, and 1 mL of the spore suspension was used to inoculate the seedlings following the procedure described by Strelkov et al. (2007); the details of this can be found in Adhikary, Mehta, et al. (2022b) and Adhikary, Kisiala, et al. (2022a).

The plants were uprooted at 50 days post inoculation (dpi) and the roots were washed thoroughly to assess disease severity. Disease symptoms were rated on a scale of 0–3, where 0 = no galls, normal roots; 1 = a few small galls on the lateral roots; 2 = moderate galling; and 3 = severe galls (Kuginuki et al., 1999). The index of disease (ID%) was calculated using the formula described in Horiruchi and Hori (1980), further modified by Strelkov et al. (2006), as $ID\% = \frac{\sum[nw]}{3T} \times 100$, where n denotes the number of plants in each score, w is the disease score between 0 and 3, and T is the total number of plants tested in the experiment. Based on these preliminary results, the Si0.5 and Si1.0 treatments were selected for further studies. In addition to ID%, root length (cm) and shoot height (cm) were also measured. Clubroot disease progression was evaluated using histology at 7-, 14-, and 21-dpi, as described in Summanwar et al. (2019). Briefly, fresh root tissues were fixed in FAA (formalin, acetic acid, and alcohol) solution for 48 h at room temperature. Root sections 2–5 cm from the proximal end were obtained and dehydrated in ethanol and toluene using a Leica TP1020 tissue processor (Leica Biosystems). These root segments were embedded in paraffin blocks, sectioned into 0.7 μ m longitudinal sections using an A0 Leica rotary microtome and fixed to glass slides overnight at 37°C. These slides were deparaffinated using ethanol-toluene washes, stained and counterstained using Hematoxylin and Eosin Y, respectively, and coverslipped using DPX mounting media (Summanwar et al., 2019).

2.3 | Sample preparation for transcriptomics and metabolomics

A total of 27 samples from the three treatments (PC, Si0.5, and Si1.0) were used for transcriptomic and metabolomic analyses at 7-, 14-, and 21-dpi. Hi-Q seedlings were grown in the soil mix previously described with/without Si amendment, inoculated with *P. brassicae*, washed thoroughly, flash-frozen in liquid nitrogen and stored at –80°C until analysis. Each biological replicate comprised five individual plants per treatment, and three biological replicates were generated from three independent experiments. A total of 27 samples were generated for transcriptomics and metabolomics analyses [3 treatments (PC, Si0.5 and Si1.0) \times 3 time points (7-, 14-, and 21-dpi) \times 3 biological replicates].

2.4 | RNA extraction, RNA-seq library preparation, and data analysis

Frozen root samples were homogenized in liquid nitrogen using a sterile, nuclease-free mortar and pestle. Total RNA was extracted using RNeasy Plant Mini Kit (Qiagen) from approximately 0.1 g of homogenized root tissue following the manufacturer's protocol. To improve the RNA yield from Si-treated root samples, the homogenized tissues were pretreated with Polyethylene Glycol 8000 (PEG8000, Sigma Aldrich) to remove secondary metabolites that interfere with the extraction (Gehrig et al., 2000). In-column DNA digestion was performed using RNase-free DNase I (Qiagen) following the manufacturer's instructions to remove contaminating DNA. RNA concentration was determined using A260/280 and A260/230 ratios obtained using a Nanodrop ND-1000 spectrophotometer (ThermoFisher). RNA integrity was analyzed using Agilent 4150 TapeStation System (Agilent), and samples with RNA integrity number (RIN) greater than 9.0 were used for library preparation and sequencing at LC Sciences.

Poly (A) RNA-seq library was prepared using Illumina's TruSeq stranded-mRNA preparation protocol, where briefly, the poly (A) tail-containing mRNA sequences were purified twice from total RNA using Dynabeads oligo (dT) (ThermoFisher). Purified poly (A) mRNA fractions were fragmented into small pieces using divalent cations at elevated temperatures, and the cDNA was synthesized using SuperScript™ II Reverse Transcriptase (Invitrogen), followed by U-labeled second strand synthesis by the dUTP method. Adaptor-ligated cDNA libraries were amplified using polymerase chain reaction (PCR), and the average 300 ± 50 bps insert size of the cDNA libraries were used for paired-end sequencing (2×150 bp) on Illumina Novaseq 6000 system following the manufacturer's protocol. Reads containing adaptor sequence, low quality and undetermined bases were removed by LC Sciences' in-house perl scripts and Cutadapt (Martin, 2011), followed by verification of the sequence quality using FastQC (<http://www.bioinformatics.babraham.ac.uk/projects/fastqc/>). HISAT2 (Kim et al., 2019) was used to align the reads to the *B. napus* ZS11 genome based on Sun et al. (2017). The mapped reads of each sample were assembled using StringTie (Pertea et al., 2015), and all the transcriptomes were merged to create a comprehensive transcriptome using gffcompare (<https://github.com/gpertea/gffcompare/>). After this, fragment per kilobase of transcript per million fragments mapped (FPKM) values were calculated using StringTie and ballgown (Pertea et al., 2016). Differential expression analysis between two treatments was performed using DESeq2 (Love et al., 2014), and between samples using edgeR (Robinson et al., 2010). Finally, only the differentially expressed genes (DEGs) that passed the threshold of $|\log_2$ fold change| ≥ 1.0 , and q -value < 0.05 were considered for further analysis.

Gene ontology (GO) and Kyoto Encyclopedia of Genes and Genomes (KEGG) databases were used for enrichment analysis of the DEGs at different time points and treatments. The DEGs were mapped to the GO terms in the database (<http://geneontology.org>) as well as the KEGG terms in the KEGG database (<http://www.genome.jp/kegg>), to determine the gene numbers associated with each term. Significant GO and KEGG terms were calculated by hypergeometric

equation, $P = 1 - \sum_{i=0}^{S-1} \frac{\binom{B}{i} \binom{TB-B}{TS-i}}{\binom{TB}{TS}}$, where TB gene number = no. of total genes with GO/KEGG annotation, TS gene number = no. of DEGs in TB , B gene number = total no. of genes annotated to certain GO terms/KEGG pathways, S gene number = no. of DEGs in S . Bonferroni correction was applied to control the error due to multiple comparisons, and those with p -value < 0.05 were defined as significant GO/KEGG terms. The rich factor (RF) for each GO/KEGG term was also calculated ($RF = S$ gene number/ B gene number).

2.5 | Quantitative real-time polymerase chain reaction (qRT-PCR) assays

Expression levels of 16 DEGs identified through the RNA-seq were validated using qRT-PCR. qRT-PCR assays were performed using gene-specific primers (Supporting Information File S3), using the reaction conditions as described in Adhikary, Kisiala, et al. (2022a) and *UBIQUITIN CONJUGATING ENZYME 9 (UBC9)* was used as the endogenous control (Summanwar et al., 2019, 2021). The cycle threshold (C_t) for each sample was determined based on three biological replicates, analyzed in two technical replications, and the relative fold change of the DEGs were calculated using the $2^{-\Delta\Delta C_t}$ method (Schmittgen & Livak, 2008).

2.6 | Extraction and quantification of phytohormones, secondary metabolites (glucosinolates), and amino acids using high performance liquid chromatography—(high resolution-accurate mass)—tandem mass spectrometry (HPLCMSMS)

Plant hormones and selected primary and secondary metabolites were profiled in PC, Si0.5, and Si1.0 root samples, harvested at 7-, 14-, and 21-dpi using approximately 0.07 g of homogenized root tissue that was flash frozen in liquid nitrogen and stored at -80°C . All profiled metabolites were extracted using a previously published method (Šimura et al., 2018) with modifications to facilitate the extraction of cytokinins (CKs), acidic hormones (abscisic acid [ABA], indole-3-acetic acid [IAA], salicylic acid [SA] and jasmonic acid [JA], primary metabolites [free AAs]), and secondary metabolites (glucosinolates) from a single plant sample. Levels of phytohormones and AAs in canola root samples were standardized to pmol g^{-1} of plant fresh weight (FW). The normalized relative levels of secondary metabolites and associated compounds were calculated based on the mean recoveries of the deuterated CK internal standards in each sample. AAs and secondary metabolites were identified by accurate mass, comparison of retention times to authentic standards or by accurate mass and comparison of fragmentation patterns to MS/MS databases (METLIN, PubChem, KEGG) (Tables S21 and S22). Additional details on the extraction and quantification of these compounds are provided in Supporting Information File S1. All data have been deposited to the Metabolomics Workbench (Sud et al., 2016) under Study ID ST002406, and can be accessed using the DOI: <https://doi.org/10.21228/M8M42M>.

2.7 | Peroxidase and catalase enzyme assays

Enzyme activities were measured for the 21 dpi samples (PC, Si0.5, and Si1.0) since there were clear differences in gall formation in the presence or absence of Si. Peroxidase (POD, EC 1.11.1.7) enzyme activity in the supernatant was determined with Peroxidase Activity Assay Kit per the manufacturer's instructions (Sigma Aldrich). Approximately 0.01 g of frozen homogenized root tissues were centrifuged thoroughly with 400 μL of assay buffer using Microfuge 20R (Beckman Coulter) at 13,000 g, 10 min, 4°C , and stored on ice until use. The standard curve was generated for 0, 1, 2, 3, 4, and 5 nmol well $^{-1}$ at 570 nm absorbance using SpectraMax M3 Multimode Plate Reader (Molecular Devices). The POD activity of the sample was measured by the amount of H_2O_2 reduced between T_{initial} and T_{final} for each sample (B), where the reaction mixture contained 2 μL enzyme extract (V), 48 μL assay buffer and 50 μL master reaction mix. The enzyme activity was calculated using $(B \times \text{sample dilution factor}) / (\text{reaction time} \times V)$ for the three biological replicates in two technical replications and reported in $\text{nmol min}^{-1} \text{mL}^{-1}$, where one unit of peroxidase is the amount of enzyme that reduces 1.0 μmol of H_2O_2 per minute at 37°C .

Similarly, for catalase (CAT, EC 1.11.1.6), the enzyme activity was determined by the depletion of H_2O_2 by monitoring the decrease in absorbance at 240 nm. The reaction mixture contained 10 μL enzyme extract, 50 mM phosphate buffer (pH 7.0) and 10 mM H_2O_2 , and the enzyme activity was calculated using the extinction coefficient $\epsilon_{240} = 40 \text{ cm}^2 \mu\text{mol}^{-1}$ (Aebi, 1974), reported in $\text{nmol min}^{-1} \text{mL}^{-1}$ for three biological replicates in two technical replications.

2.8 | Statistical analyses

Statistical analyses were conducted using the Microsoft Excel and the R-studio software (v. 4.2.1, 2022-06-23). The root lengths and plant height data from independent experiments were tested for normality by a Shapiro-Wilk's test using the dplyr library R-package and homogeneity of variance using Levene's test available under car R-package. Since they exhibited homogeneity, the data from independent experiments were combined and represented as mean \pm standard error (se). The heatmaps were generated using pheatmap R-package and were scaled by rows. All t-tests for the comparison of means were conducted between PC and Si-treatment at respective timepoint using T.TEST() in Excel, where $p < 0.05$ was considered statistically significant unless otherwise stated.

3 | RESULTS

3.1 | Clubroot disease severity in the presence/absence of Si

We evaluated the effects of different concentrations of silicon (Si) on clubroot disease severity (average disease index $\text{ID}\% \pm \text{se}$; Figure 1A). Among the different concentrations, the highest amount of Si amendment, Si1.0, resulted in partial resistance to clubroot with an $\text{ID}\%$ of

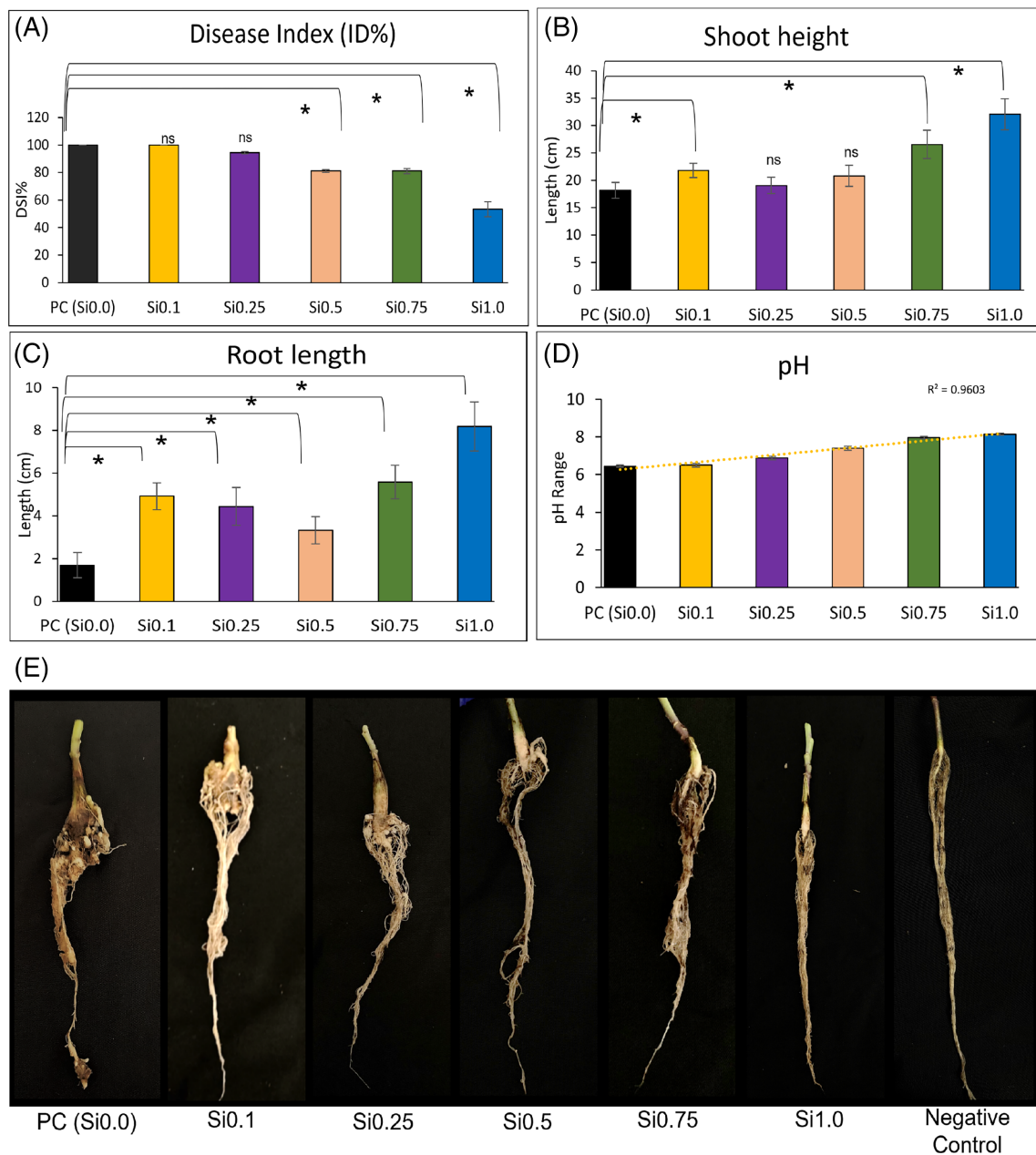


FIGURE 1 Evaluation of plant parameters due to Si treatment in presence of *Plasmodiophora brassicae*. The (A) disease index (ID)%, (B) shoot height, (C) root length, (D) pH of the soil mixes, and (E) representative root images for all Si-treated plants measured 50 days post infection (dpi) with *P. brassicae*. Error bars denote standard error of mean of parameters from three experimental replications, comprising of total 30 plants. Statistical significance for each Si-treatment calculated in comparison to “pathogen control (PC)” using Student’s *t*-test, denoted by the bar with “***” ($p < 0.05$), treatments PC (Si0.0)—0.0 g Si (control), Si0.1—0.1 g Si (Si:soil in 1:1000, w/w), Si0.25—0.25 g (Si:soil in 1:400, w/w), Si0.5—0.5 g (Si:soil in 1:200, w/w), Si0.75—0.75 g (Si:soil in 3:400, w/w), and Si1.0—1.0 g (Si:soil in 1:100, w/w), mixed with 100 g of soil-mix and inoculated with *P. brassicae*.

54% ($p < 0.01$), while the moderate amounts, Si0.5 and Si0.75 caused mild susceptibility with an ID% of 83–80% ($p < 0.05$). The plants grown in lower Si concentrations, Si0.1 and Si0.25, were completely susceptible to clubroot disease with an ID% of 95–100%. Since we used a highly susceptible variety (Hi-Q) in all experiments, the PC (Si0.0) exhibited complete susceptibility to clubroot with an ID% of 100%.

The overall plant health was evaluated by measuring the shoot height and root length at the end of the experiment, that is, 50 dpi. Si

treatment improved shoot height for all treatments (Figure 1B) and was statistically significant ($p < 0.05$) for Si0.1, Si0.75, and Si1.0 treatments, while the root lengths were significantly ($p < 0.05$) greater for all Si treatments (Figure 1C). The average pH of the soil mix ranged from 6.50 to 8.14; this demonstrated a trend of increasing pH with the increase in Si concentration (Figure 1D). Representative root images for all treatments (with/without Si amendment) are presented in Figure 1E. Based on this, the treatments Si0.5 and Si1.0, with pH of

7.39–8.14 were selected for subsequent studies since they exhibited a reduction in clubroot disease symptoms.

3.2 | Microscopic examination of disease progression in the presence/absence of Si

Microscopic examination of root sections from plants on day 7 in the PC, Si0.5, and Si1.0 indicated no differences in pathogen developmental stages. The primary infection of *P. brassicae* was successful irrespective of Si application at 7 dpi, as indicated by the presence of primary zoospores in all three treatments (Figure 2A–C). At 14 dpi, we observed an overall progression of the infection where the zoospores had invaded further into the cortical section of the roots. Specifically, in the case of PC (Figure 2D), mature and sporulating secondary plasmodia were observed in the cortical cells, whereas in Si0.5, a larger number of resting spores and a few mature secondary plasmodia were present in many cells, as indicated by the arrows (Figure 2E). In case of Si1.0, mainly resting spores were present in some cortical cells at 14 dpi (Figure 2F).

At 21-dpi, a clear distinction in gall development stages could be observed at the macroscopic level. The PC plants showed symptoms of clubroot severity, while for Si0.5, the severity of galling was visibly reduced and was lowest for Si1.0 treatment (Figure 2J–L). At the microscopic level, clusters containing mature secondary plasmodia stacked in the cortex region were present in PC plants (Figure 2G), whereas a combination of smaller clusters of mature secondary plasmodia and resting spores were observed in the cortical cells of Si0.5 plants (Figure 2H). Finally, only a few resting spores were observed in the cortical cells of Si1.0 plants (Figure 2I). Based on these observations, 7-, 14-, and 21-dpi were selected for transcriptomics and metabolomics.

3.3 | Effects of Si on *P. brassicae*-induced transcriptome-level changes in *B. napus* roots

To elucidate the role of Si in mediating resistance against *P. brassicae*, the transcriptomic responses of clubroot-infected roots with/without Si were investigated. Transcripts were sequenced from 27 samples comprising the three biological replicates of PC, Si0.5, and Si1.0 at 7-, 14-, and 21-dpi. This resulted in an average of 43,899,980 clean reads per sample with a minimum of 37,573,196 reads and a maximum of 54,349,198 reads (Table S1). The Q20% and Q30% values of all samples were $\geq 95\%$, indicating that the data was accurate and reliable, and $\geq 81\%$ of the reads were mapped to the reference genome of *B. napus* ZS11 as developed by Sun et al. (2017).

For differentially expressed genes (DEGs), the absolute \log_2 fold change (fc) > 1.0 , and false rate discovery (FDR) denoted by “q-value” was at 95% confidence ($q < 0.05$) among the treatments. Between Si0.5 and PC plants, we identified 805, 2085, and 3917 DEGs at 7-, 14-, and 21-dpi, respectively (Figure 3A, Tables S7–S9). When Si1.0 and PC root tissues were compared, 1535, 5721, and 6825 genes

were differentially expressed at the three respective time points (Figure 3A, Tables S10–S12), marking an increase in transcript-level responses due to higher Si concentration.

A total of 19 DEGs were common among the two comparisons (Si0.5 vs. PC and Si1.0 vs. PC) at all three time points. Among the common DEGs exhibiting consistent expression patterns, there was an elevated response (greater upregulation or downregulation) with the higher Si treatment (Si1.0) as opposed to Si0.5 at any time point with a maximum \log_2 fc of 5.77 and minimum \log_2 fc of -4.76 (Table S2). Additionally, a number of DEGs were upregulated due to Si treatment alone (observed fragment per kilobase million (FPKM) value in PC was 0.00), which were considered “unique” due to Si treatments. There were 26, 50, and 108 DEGs between Si0.5 versus PC, while between Si1.0 versus PC, 36, 105, and 224 DEGs were uniquely upregulated at the three time points (Figure 3B, Table S13). These results indicate that both Si0.5 and Si1.0 treatments elicit gene expression changes in the presence of the pathogen, and these changes may be involved in ameliorating the severity/progression of the disease.

3.3.1 | GO and KEGG enrichment of the DEGs

To identify the metabolic pathways altered due to Si treatment during *B. napus*–*P. brassicae* interactions, functional categorization of the DEGs identified in the two comparisons were carried out using both KEGG and GO databases. Enrichment of the DEGs in the KEGG database exhibited a total of 66 unique metabolic process significantly ($p < 0.05$) enriched at least at one time point and treatment. Among them, “ko04626: Plant pathogen interactions,” “ko04075: Plant hormone signal transduction” and “ko04016: MAPK signalling pathway in plants” were the top common over-represented categories for both treatments at all three time points (Figure 3C–H, Table S5). We also observed “ko00940: Phenylpropanoid biosynthesis,” “ko00500: Starch and sucrose metabolism,” “ko00960: Glucosinolate biosynthesis,” and “ko00910: Nitrogen metabolism” to be some of the highly enriched terms at least at two time points in both treatments (Figure 3C–H, Table S5). In subsequent sections, we have focused primarily on the DEGs and metabolites associated with the aforementioned highly enriched biological processes. Additional findings on GO and KEGG analysis are described in Supporting Information File S2.

3.4 | Effects of Si on *P. brassicae*-induced expression of specific genes involved in host-pathogen interaction

3.4.1 | Antioxidant enzymes

We observed several DEGs related to antioxidant enzymes (*POD*, *CAT*, *SOD*) summarized in Table 1. Their expression levels are presented in Figure 4A and Table S14.

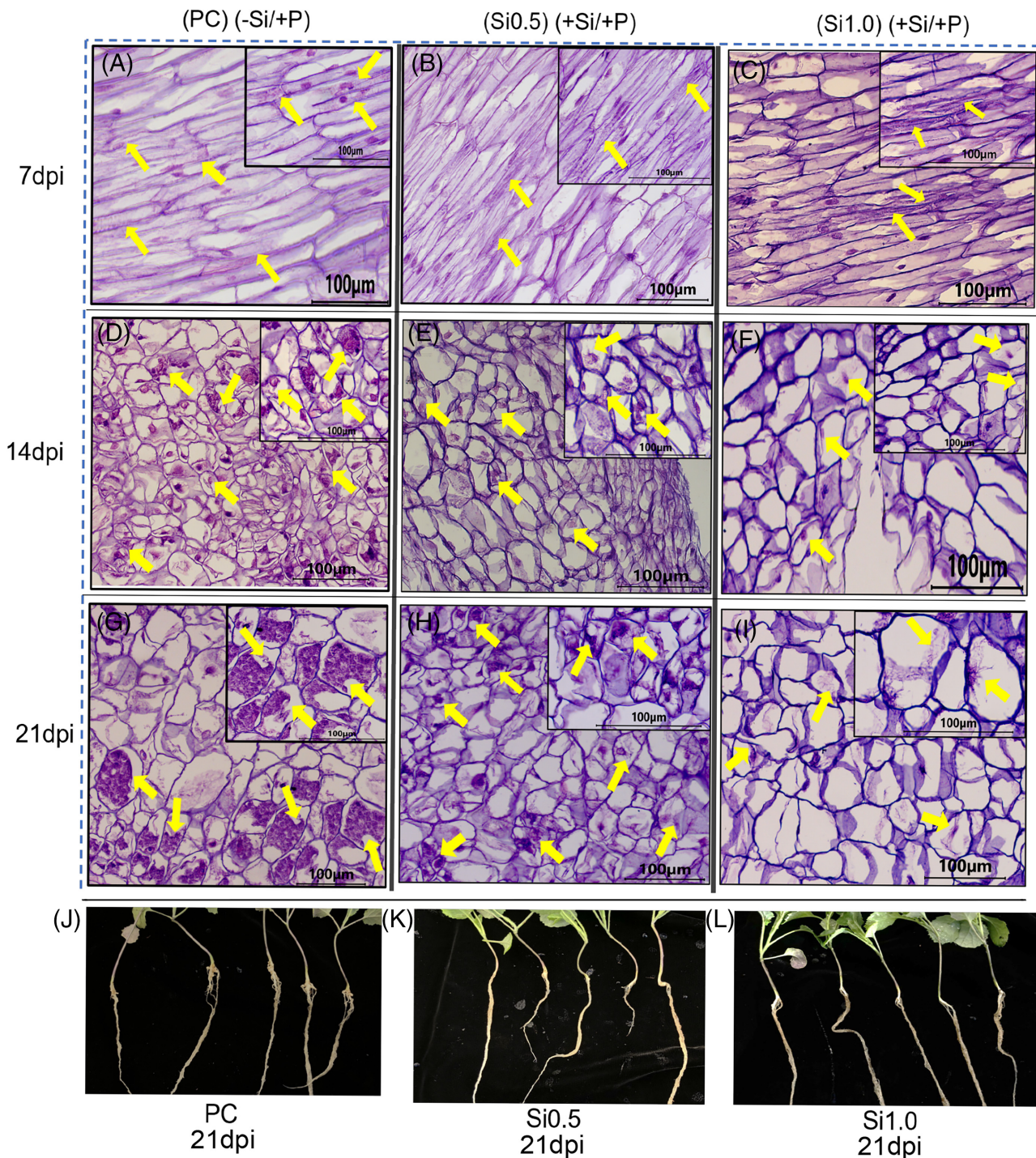


FIGURE 2 Microscopic appearance of *P. brassicae*-infected *B. napus* roots stained with Hematoxylin and Eosin, collected at 7-, 14-, and 21-days post infection (dpi) and the appearance of seedling roots at 21-dpi in the presence or absence of silicon. Presence of primary infection at 7-dpi (A–C), indicated by yellow arrows, denotes infection by *P. brassicae* in all treatments. The gradual advancement of infection at 14- and 21-dpi is indicated by the presence of mature secondary plasmodia in several cortical tissues of PC (D,G), whereas Si1.0 and Si0.5 shows reduced progression of infection (E, F, H, I), observed at 20X and 40X magnification. Root phenotypes for PC, Si0.5, and Si1.0 seedling roots at 21 dpi are shown in J–L.

3.4.2 | Systemic responses associated with defence hormones

Several transcripts related to defence hormones signalling, such as SA (*NPR1*, *TGA*, *WRKY29*), JA (*JAZ*), and ET (*EIN3*, *EBF2*) have been

identified and summarized in Table 1. In addition, two transcripts related to defensins *PDF1.2* (KO: K20727) were consistently upregulated. One (*BnC02g0498540.1*) was upregulated at both 14- and 21-dpi (Si0.5) and 7 dpi (Si1.0), while another transcript (*BnC01g0425010.1*) was upregulated at 21 dpi (Si0.5) and at both 7- and 21-dpi (Si1.0) (Figure 4B, Table S15).

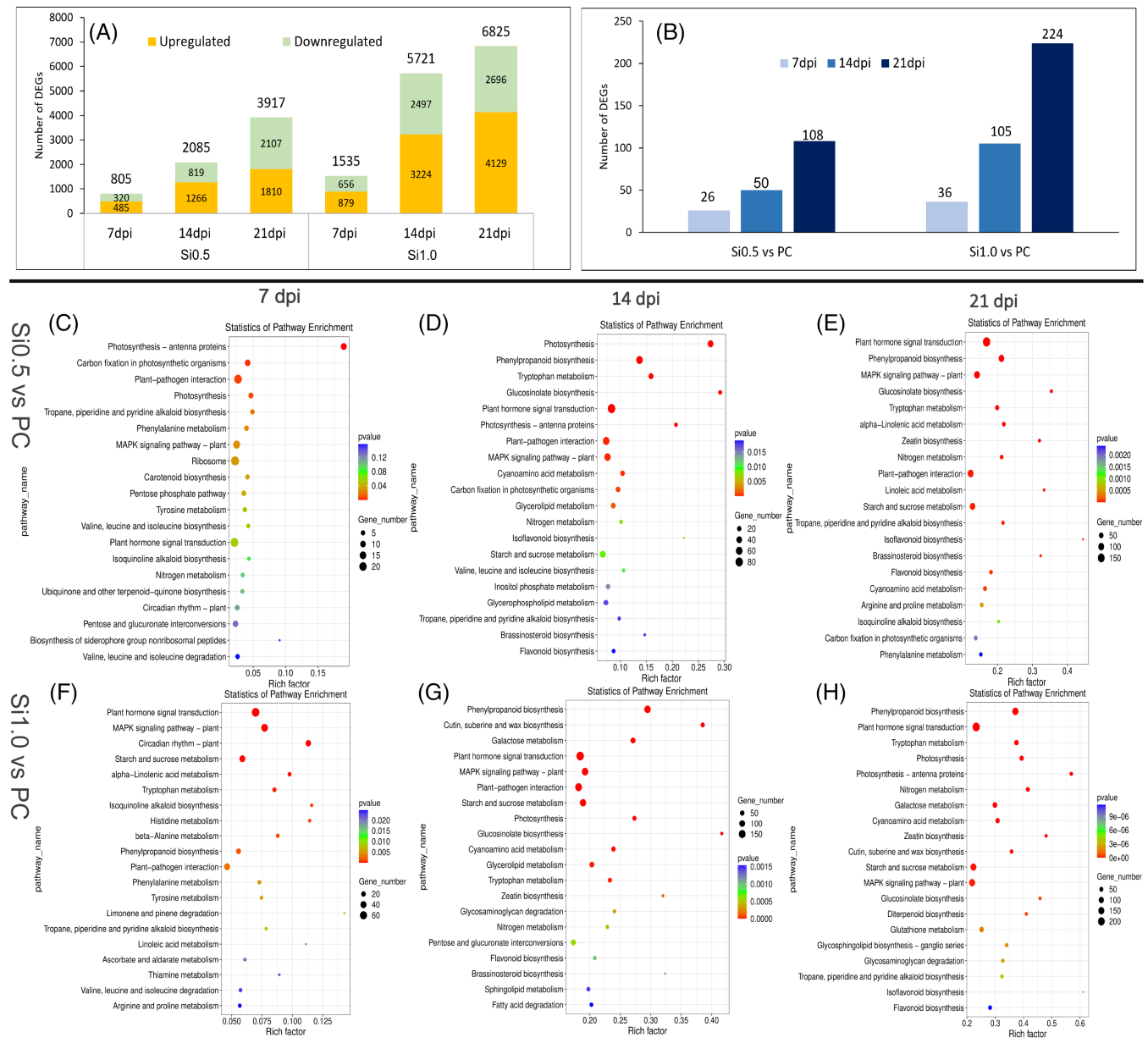


FIGURE 3 (A) Differentially expressed genes (DEGs), upregulated and downregulated, at 7-, 14-, and 21-days post infection (dpi) due to Si-treatments during *B. napus* and *P. brassicae* interaction. (B) DEGs uniquely upregulated (fragments per kilobase million or FPKM = 0.00 for PC) due to silicon treatments at the three time points during host-pathogen interactions. The top 20 Kyoto Encyclopedia of Genes and Genomes (KEGG) enriched terms for the DEGs in response to Si0.5 (C–E) and Si1.0 (F–H) treatment respectively, when compared to the control (PC) at the three time points. All DEGs with q -value < 0.05 and $|\log_2$ fold change| > 1.000 were considered, treatments PC (Si0.0)—0.0 g Si (control); Si0.5—0.5 g Si; and Si1.0—1.0 g Si in 100 g soil-mix, inoculated with clubroot pathogen.

3.4.3 | Metabolism and signal transduction of IAA and CKs

Many DEGs related to IAA biosynthesis (*TAA*, *YUCCA*) and signalling (*AUX1*, *SAUR*) mechanisms have been identified and highlighted in Table 1. Additionally, we detected a total of 23 transcripts associated with growth hormone (*GH*) (KO: K14487) related to IAA signalling (Table S16). Among them, three *GH*-related genes (*BnA02g0051360.1*, *BnC03g0540680.1*, and *BnC09g0888070.1*) were consistently downregulated in at least one time point for Si0.5 and all three time points

in Si1.0 plants, while two (*BnA09g0343600.1* and *BnC01g0445940.1*) were upregulated at 14- and 21- dpi in both Si treatments (Figure 4C, Table S16).

Several transcripts associated with CK metabolism (*IPT*, *CYP735A*, *CKX*), as well as signal transduction (*HK1*, *ARR-B*, and *ARR-A*), were identified (Figure 4C, Table S16) and summarized in Table 1. Among the 36 DEGs related to *ARR-B*s, one (*BnC03g0605470.1*) showed downregulation at 7 dpi in both Si treatments, followed by upregulation at 14- and 21-dpi (Si0.5) and 21 dpi (Si1.0) (Figure 4C, Table S16).

TABLE 1 Summary of specific genes modulated during host pathogen interactions due to Si treatment on *P. brassicae*-challenged *B. napus* roots at 7-, 14-, and 21-days post infection.

Metabolic processes	Gene symbol	Identifier	Total number of transcripts identified	DEGs with consistent expression (up/down) ($q < 0.05$ and $ \log_2 \text{fold} > 1.0000$)		
				Up	Down	Timepoints and treatments
Antioxidant related	<i>POD</i>	EC:1.11.1.7	76	8	1	Si0.5 and Si1.0 (14- and 21-dpi)
	<i>CAT</i>	EC 1.11.1.6	10	1	1	Si0.5 and Si1.0 (14- and 21-dpi)
	<i>SOD</i>	EC:1.15.1.11	6	-	3	Si0.5 and Si1.0 (7 dpi)
Defence hormone signaling related	<i>NPR1</i>	KO:K14508	1	-	1	Si0.5 (14 dpi) and Si1.0 (14- and 21-dpi)
	<i>NPR5/6</i>	KO:K14508	5	5	-	Si1.0 (21-dpi)
	<i>WRKY29</i>	KO:K13426	2	1	-	Si0.5 (21-dpi) and Si1.0 (7-, 14-, and 21-dpi)
	<i>TGA</i>	KO:K14431	23	3	-	Si0.5 and Si1.0 (14- and 21-dpi)
	<i>JAZ</i>	KO:K13464	34	-	12	Si0.5 and Si1.0 (21 dpi)
	<i>EBF1/2</i>	KO:K14515	2	2	-	Si0.5 (21 dpi) and Si1.0 (7 dpi)
	<i>EIN3</i>	KO:K14514	7	4	1	Si0.5 and Si1.0 (21 dpi)
Metabolism and signal transduction of IAA and CKs	<i>TAA</i>	EC:2.6.1.99	6	1	-	Si0.5 and Si1.0 (14- and 21-dpi)
	<i>YUCCA</i>	EC:1.14.13.168	19	2	-	Si0.5 and Si1.0 (14- and 21-dpi)
	<i>PIN2</i>	NA	2	2	-	Si0.5 and Si1.0 (14- and 21-dpi)
	<i>AUX1</i>	KO:K13946	6	3	-	Si0.5 and Si1.0 (21 dpi)
	<i>SAUR</i>	KO:K14488	31	1	-	Si0.5 and Si1.0 (14- and 21-dpi)
	<i>IPT</i>	EC:2.5.1.27; EC:2.5.1.112	7	4	-	Si0.5 and Si1.0 (21 dpi)
	<i>CYP735A</i>	KO:K10717	1	1	-	Si0.5 (21 dpi) and Si1.0 (14- and 21-dpi)
	<i>CKX</i>	EC:1.5.99.12	9	-	1	Si1.0 (7-, 14-, and 21-dpi)
	<i>HK1</i>	EC:2.7.13.3	6	1	-	Si0.5 and Si1.0 (14- and 21-dpi)
	<i>ARR-B</i>	KO:K14491	36	2	-	Si0.5 and Si1.0 (14- and 21-dpi)
	<i>ARR-A</i>	KO:K14492	16	2	-	Si0.5 and Si1.0 (21 dpi)
	ABA related	<i>PYR/PYL</i>	KO:K14496	21	2	-
<i>SnRK2</i>		K14498	12	2	2	Si0.5 and Si1.0 (21 dpi)
<i>DHN</i>		NA	3	3	-	Si0.5 (14- and 21-dpi) and Si1.0 (21 dpi)
Nitrogen metabolism and transport	<i>NRT</i>	K02575	6	1	-	Si0.5 and Si1.0 (7-, 14-, and 21-dpi)
	<i>NRT</i>	NA	5	5	-	Si0.5 and Si1.0 (14- and 21-dpi)
	<i>AAP8</i>	NA	2	2	-	Si0.5 and Si1.0 (21 dpi)
	<i>AAP4</i>	NA	4	4	-	Si1.0 (14- and 21-dpi)
	<i>AAT</i>	EC:2.6.1.1	4	4	-	Si0.5 and Si1.0 (21 dpi)
	<i>GDH</i>	EC:1.4.1.3	6	3	-	Si0.5 and Si1.0 (21 dpi)

(Continues)

TABLE 1 (Continued)

Metabolic processes	Gene symbol	Identifier	Total number of transcripts identified	DEGs with consistent expression (up/down) ($q < 0.05$ and $ \log_2 \text{fold} > 1.0000$)		
				Up	Down	Timepoints and treatments
Biosynthesis of secondary metabolites	<i>BCAT4</i>	K21346	4	4	-	Si0.5 (14- or 21-dpi) and Si1.0 (14- and 21-dpi)
	<i>CYP79F1/2</i>	EC:1.14.14.42	1	1	-	Si0.5 and Si1.0 (14- and 21-dpi)
	<i>CYP79B1/2</i>	K11812	2	-	2	Si0.5 and Si1.0 (21 dpi)
	<i>ST/SOT</i>	K22321	5	2	-	Si0.5(21 dpi) and Si1.0 (14- and 21-dpi)
	<i>PAL</i>	EC:4.3.1.24	1	1	-	Si1.0 (21 dpi)
	<i>CHS</i>	EC:2.3.1.74	1	1	-	Si0.5 (21 dpi) and Si1.0 (7-, 14-, and 21-dpi)
	<i>HCT</i>	EC:2.3.1.133	4	1	-	Si0.5 (21 dpi) and Si1.0 (14- and 21-dpi)
	<i>CCOAOMT</i>	EC:2.1.1.104	6	-	1	Si0.5 and Si1.0 (14- and 21-dpi)
	<i>FLS</i>	EC:1.14.20.6	14	4	5	Si0.5 and Si1.0 (21 dpi)
	<i>UDP-glu</i>	EC:2.4.1.111	1	1	-	Si1.0 (14- and 21-dpi)

Note: The total number of transcripts detected for each gene are listed in column 4, the number of transcripts in columns 5 and 6 indicate those that are consistently up or down regulated, respectively, and column 7 indicates the treatments and time points which resulted in that consistent regulation of expression.

Abbreviations: *POD*, peroxidase; *CAT*, catalase; *SOD*, superoxide dismutase; *NPR1*, non-expressor of pathogenesis related-1; *NPR5/NPR6*, non-expressor of pathogenesis related-5/6; *WRKY29*, WRKY transcription factor 29; *TGA*, transcription factor TGA; *JAZ*, jasmonate ZIM domain-containing protein; *EBF1/2*, EIN3-binding F-box protein; *EIN3*, ethylene-insensitive protein 3; *TAA*, L-tryptophan, -pyruvate aminotransferase; *YUCCA*, indole-3-pyruvate monooxygenase; *PIN2*, auxin efflux carrier component 2-like; *AUX1*, auxin influx carrier; *SAUR*, SAUR family protein; *IPT*, adenylate isopentenyl transferase; *CYP735A*, cytokinin trans-hydroxylase; *CKX*, cytokinin dehydrogenase; *HK1*, histidine kinase; *ARR-B*, two-component response regulator ARR-B family; *ARR-A*, two-component response regulator ARR-A family; *PYR/PYL*, abscisic acid receptor PYR/PYL family; *SnRK2*, serine/threonine-protein kinase SRK2; *DHN*, dehydrin Rab-18 isoform; *NRT*, nitrate/nitrite transporter; *AAP8*, amino acid permease 8; *AAP4*, amino acid permease 4; *AAT*, aspartate aminotransferase; *GDH*, glutamate dehydrogenase; *BCAT4*, branched chain aminotransferase 4 (methionine transaminase); *CYP79F1/2*, homomethionine N-monooxygenase; *CYP79B1/2*, tryptophan N-monooxygenase; *ST/SOT*, aliphatic desulfoglucosinolate sulfotransferase; *PAL*, phenylalanine ammonia-lyase; *CHS*, chalcone synthase; *HCT*, shikimate O-hydroxycinnamoyltransferase; *CCOAOMT*, coffeoyl-CoA O-methyltransferase; *FLS*, flavonol synthase; *UDP-glu*, UDP-glucose coniferyl alcohol glucosyltransferase.

3.4.4 | Abscisic acid (ABA) related

Transcripts associated with ABA signalling (*PYR/PYL*, *SnRK2*) as well as abiotic stress-responsive dehydrins were differentially expressed due to Si-treatment and have been summarized in Table 1. Among them, one dehydrin (*BnCO2g0529880.1*) was consistently upregulated for all three time points for the Si0.5 treatment (Figure 4D, Table S16).

3.4.5 | Nitrogen metabolism and transport

We observed several DEGs associated with nitrogen transportation (*NRT*, *AAP*) and assimilation (*AAT*, *GDH*), summarized in Table 1. In addition, eight transcripts related to *glutamine synthetase* (*GS*) (EC:6.1.3.2), which converts AA glutamate to glutamine during N-fixation, were identified, and one (*BnA02g0064060.1*) was downregulated at 7 dpi (Si0.5), followed by upregulation at 14- and 21-dpi for both Si treatments (Figure 4E, Table S17).

3.4.6 | Biosynthesis of secondary metabolites

The phenylpropanoid and glucosinolate biosynthesis pathways were enriched at 14- and 21-dpi in both Si treatments. We identified transcripts related to the phenylpropanoid biosynthesis pathway (*PAL*, *HCT*, *FLS*) and glucosinolate biosynthesis genes (*BCAT4*, *CYP79F1/2*, and *CYP79B1/2*; Figure 4F, Table S18), and have been summarized in Table 1.

3.5 | Validation of the NGS results using qRT-PCR

A total of 16 DEGs were selected for validation using qRT-PCR, some of which have been highlighted in Figure 4. These include genes related to SA-mediated signal transduction, JA-ET responsive signalling, ABA signalling pathway, nitrogen metabolism and transport, and genes related to the biosynthesis of secondary metabolites. The gene expression, evaluated by qRT-PCR, was generally consistent with the

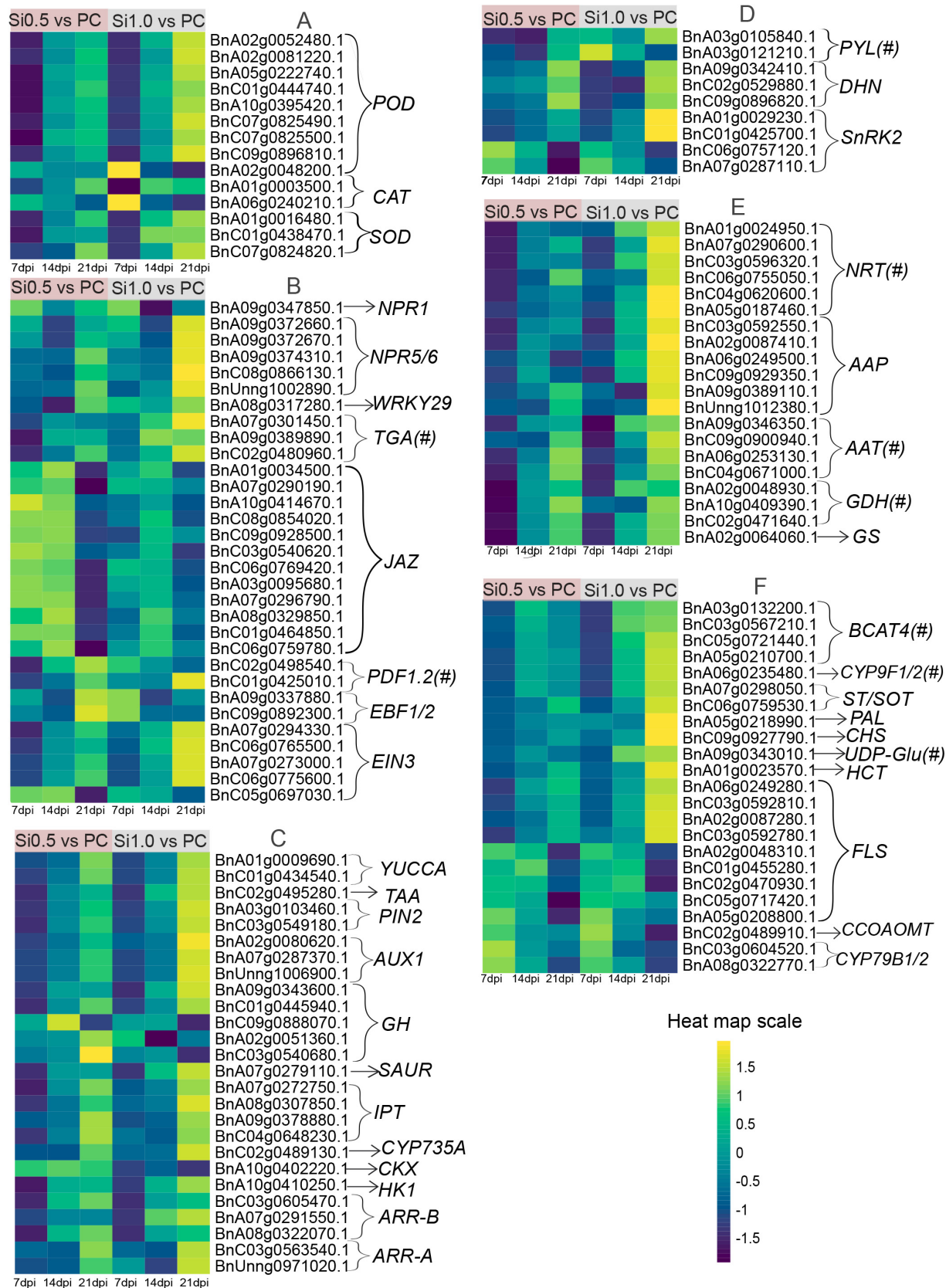


FIGURE 4 Legend on next page.

results from NGS (Supporting Information File S3) and validated the reliability of transcriptomics results.

3.6 | Effects of Si on *P. brassicae*-induced metabolite profiles in canola roots

3.6.1 | Si-induced changes to endogenous phytohormone profiles in pathogen-challenged root tissues

Several phytohormones play vital roles in clubroot disease progression. In our study, we detected stress-related phytohormones such as salicylic acid (SA), jasmonic acid (JA) and abscisic acid (ABA) (Figure 5A–C). The endogenous levels of these stress hormones were higher in PC compared to the Si-treated (Si0.5 and Si1.0), particularly at 14- and 21-dpi (Table 2). We also identified growth-promoting hormones such as auxin (IAA) and cytokinin (CKs) (Figure 5D,E). Their levels in Si0.5 and Si1.0 were increased at 7-dpi, followed by a decrease at the later time points compared to PC (Table 2).

3.6.2 | Changes in AA and secondary metabolite profiles

Amino acids

The transcriptome-level observations indicated that DEGs associated with nitrogen metabolism were enriched in Si0.5- and Si1.0-treated plants at 14- and 21-dpi; therefore, we analyzed the endogenous profiles of the free AA. Fifteen AAs were detected, exhibiting various trends following the Si treatments in pathogen-challenged root tissues (Table S19). Most AAs were increased at 7-dpi, after which their levels decreased compared to PC. Specifically, seven AA (phenylalanine, leucine, methionine, *iso*-leucine, tyrosine, threonine, and valine) were consistently decreased for both Si0.5 and Si1.0 plants at 14- and 21-dpi (Figure 6A–G). Glutamine levels were the highest in the analyzed

samples compared to other AAs and ranged between 140 and 4900 pmol g⁻¹ FW. In contrast to the trend above, endogenous glutamine levels were significantly ($p < 0.05$) lower at 7-dpi in Si-treated plants, while they were increased in Si-treated samples at 21-dpi when compared to PC (Figure 6H).

Secondary metabolites

Plants defend themselves against phytopathogens through the biosynthesis of diverse secondary metabolites, including glucosinolates (reviewed by Jan et al., 2021). Several DEGs related to phenylpropanoid and glucosinolate biosynthesis pathways were modulated due to Si treatment based on transcriptomics. In this case, we detected 22 secondary metabolites and their intermediates altered in the clubroot-infected roots due to Si application (Table S19). Like AAs, most of these secondary metabolites were higher at 7 dpi, followed by a decrease at 14- and 21-dpi in the Si-treated samples. Two metabolites, syringin and coniferin biosynthesized via the phenylpropanoid pathway, showed a similar pattern of lower accumulation at 21-dpi (coniferin, not significant; Figure 6J,L). Similarly, Si-treated plants had significantly ($p < 0.05$) higher levels of glucosinolate, 4-methoxyindole-3-carboxaldehyde, at 7-dpi compared to PC plants. A subsequent decline in endogenous levels at later time points was observed for glucosinolates brassicanal, rutalexin, 4-methoxyindole-3-carboxaldehyde, and indole-3-carboxaldehyde (Figure 6K,M–O). In contrast, other glucosinolates, such as brassicanate A, were significantly ($p < 0.01$) elevated in the 21-dpi Si-treated plants (Figure 6P). Others, such as brassinin, gluconasturiin, dihydroneoascorbigen, and indole-3-acetonitrile were also increased at 21-dpi, but the changes were not significant (Table S19).

3.7 | Antioxidant enzyme activities

We observed differential expression of *POD* and *CAT* genes in the Si-treated root samples; hence, we determined the total activities of these two enzymes in the 21 dpi samples. The activity of *POD* in the

FIGURE 4 Heatmaps representing consistent expression profiles of differentially expressed genes (DEGs) related to different biological processes altered due to Si-treatment during *P. brassicae* interaction with *B. napus*: (A) Antioxidant enzymes; (B) Salicylic Acid (SA), Jasmonic Acid (JA), and Ethylene (ET) signalling; (C) Auxin (indole-3-acetic acid, IAA) and Cytokinin (CK)-biosynthesis and metabolism; (D) Abscisic acid (ABA)- related; (E) Nitrogen metabolism and transport; (F) Biosynthesis of secondary metabolites, heatmaps scaled by rows. Symbol “#” denotes at least one transcript related to the specific gene has been validated using qRT-PCR, treatments PC (Si0.0)—0.0 g Si (control), Si0.5—0.5 g Si, and Si1.0—1.0 g Si in 100 g soil-mix, inoculated with clubroot pathogen. Gene names: *AAP*, amino acid permease; *AAT*, aspartate aminotransferase; *ARR-A*, two-component response regulator ARR-A family; *ARR-B*, two-component response regulator ARR-B family; *AUX1*, auxin influx carrier; *BCAT4*, branched chain aminotransferase 4 (methionine transaminase); *CAT*, catalase; *CCOAMT*, caffeoyl-CoA O-methyltransferase; *CHS*, chalcone synthase; *CKX*, cytokinin dehydrogenase; *CYP735A*, cytokinin trans-hydroxylase; *CYP79B1/2*, tryptophan N-monooxygenase; *CYP79F1/2*, homomethionine N-monooxygenase; *DHN*, dehydrin Rab-18 isoform; *EBF1/2*, EIN3-binding F-box protein; *EIN3*, ethylene-insensitive protein 3; *FLS*, flavonol synthase; *GDH*, glutamate dehydrogenase; *GH*, growth hormone; *GS*, glutamine synthetase; *HCT*, shikimate O-hydroxycinnamoyltransferase; *HK1*, histidine kinase; *IPT*, adenylate isopentenyl transferase; *JAZ*, jasmonate ZIM domain-containing protein; *NPR1*, non-expressor of pathogenesis related-1; *NPR5/NPR6*, non-expressor of pathogenesis related-5/6; *NRT*, nitrate/nitrite transporter; *PAL*, phenylalanine ammonia-lyase; *PDF1.2*, defensins; *PIN2*, auxin efflux carrier component 2-like; *POD*, peroxidase; *PYR/PYL*, abscisic acid receptor PYR/PYL family; *SAUR*, SAUR family protein; *SnRK2*, serine/threonine-protein kinase SRK2; *SOD*, superoxide dismutase; *ST/SOT*, aliphatic desulfoglucosinolate sulfotransferase; *TAA*, L-tryptophan-pyruvate aminotransferase; *TGA*, transcription factor TGA; *UDP-glu*, UDP-glucose coniferyl alcohol glucosyltransferase; *WRKY29*, WRKY transcription factor 29; *YUCCA*, indole-3-pyruvate monooxygenase.

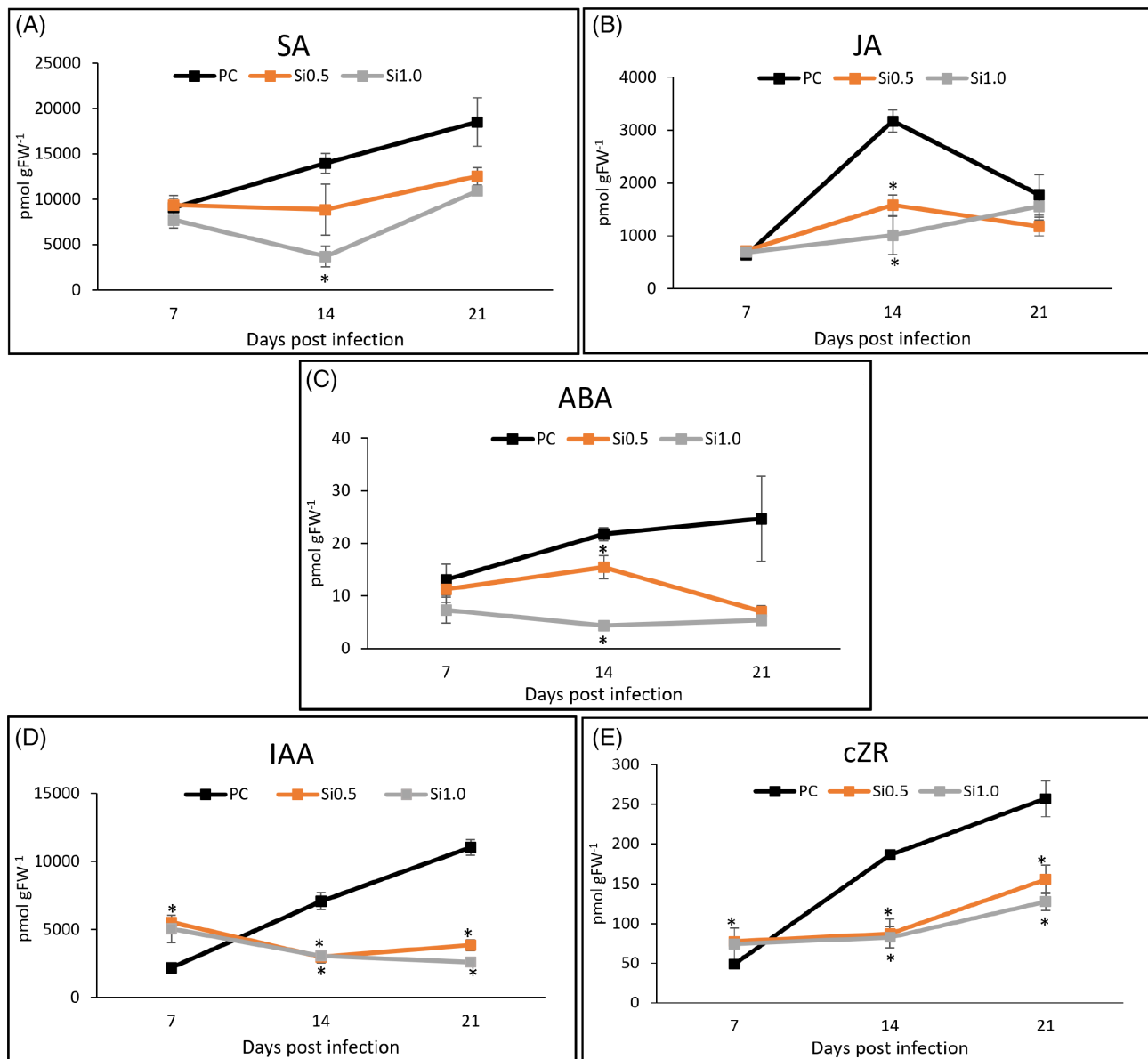


FIGURE 5 Endogenous levels of phytohormones in clubroot infected root tissues, in the presence or absence of silicon: (A) Salicylic Acid (SA), (B) Jasmonic Acid (JA), (C) Abscisic Acid (ABA), (D) Auxin (indole-3-acetic acid, IAA), and (E) Cytokinin (*cis*-Zeatin riboside, cZR), concentrations are in pmol gFW⁻¹. Error bars denote standard error of mean of three biological replicates, statistical significance ($p < 0.05$, “**”) tested using Student’s *t*-test, compared between PC and respective Si-treatment for each time point, treatments PC (Si0.0)–0.0 g Si (control), Si0.5–0.5 g Si, and Si1.0–1.0 g Si in 100 g soil-mix, inoculated with clubroot pathogen.

Si-treated samples was lower, with significantly ($p < 0.1$) reduced levels in Si1.0 plants, compared to PC (Figure 7A). Similarly, the Si-treated plants showed a significant reduction in CAT levels on 21 dpi (Figure 7B).

4 | DISCUSSION

Several reports describe the potential of Si in ameliorating plant stress, including disease responses (Feng et al., 2021; Ghareeb et al., 2011; Gou et al., 2022; Xue et al., 2021). However, there are

no reports on whether clubroot disease in canola can be mitigated by Si treatment. Clubroot control relies heavily on resistant cultivars, while soil amendments with lime have reduced clubroot symptoms (Fox et al., 2022). In this study, we conducted greenhouse experiments to demonstrate that applying Si reduces clubroot disease symptoms at the macroscopic and microscopic levels. To determine a possible mechanism of action for the observed Si-mediated protection of canola, we investigated Si-induced changes in gene expression, phytohormones, as well as primary and secondary metabolite profiles in plants challenged with the clubroot pathogen, *P. brassicae*. The performed analyses resulted in the identification of

TABLE 2 Summary of phytohormone levels modulated by Si-treatment on clubroot infected plants at 7-, 14-, and 21-dpi.

Type of phytohormone	Endogenous level range (pmol g ⁻¹ FW)	Trend across timepoints [7-, 14-, and 21-dpi]	
		Control (PC, no Si)	Si- treated [Si0.5 and Si1.0]
Stress related	SA	3703–18,514	Gradual increase with time. Lower accumulation at 14- and 21-dpi; ($p < 0.05$ for Si1.0, 14-dpi).
	JA	636–3169	Increase with time, peak at 14-dpi. Lower accumulation ($p < 0.05$ for Si0.5 and Si1.0, 14-dpi).
	ABA	4–25	Gradual increase with time. Lower accumulation ($p < 0.05$ for Si0.5 and Si1.0, 14-dpi).
Growth-promoting	IAA	2184–11,028	Gradual increase with time, lower than Si-treated plants at 7-dpi. Higher than PC at 7 dpi ($p < 0.05$ for Si0.5), decreased at later stages ($p < 0.05$ for Si0.5 and Si1.0, 14-, and 21-dpi).
	CK (cZR type)	49–257	Gradual increase with time, lower than Si-treated plants at 7-dpi. Higher than PC at 7 dpi ($p < 0.05$ for Si0.5), decreased at later stages ($p < 0.05$ for Si0.5 and Si1.0, 14-, and 21-dpi).

Abbreviations: ABA, abscisic acid; CK, cytokinin; cZR, *cis* Zeatin Riboside; IAA, auxin; JA, jasmonic acid; SA, salicylic acid.

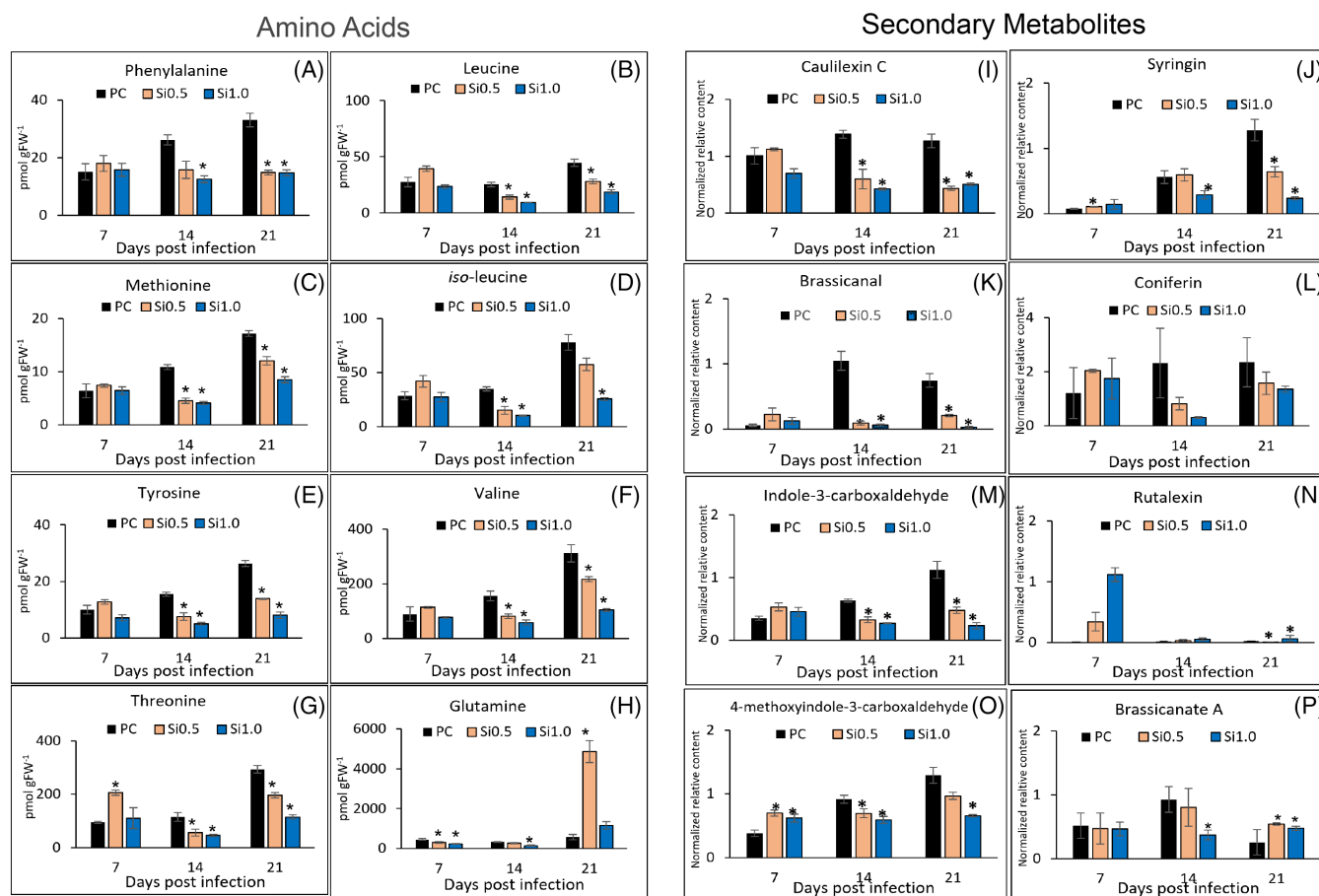


FIGURE 6 Endogenous levels of amino acids in the clubroot infected tissues, in the presence and absence of silicon: (A) Phenylalanine; (B) Leucine; (C) Methionine; (D) *iso*-leucine; (E) Tyrosine; (F) Valine; (G) Threonine; (H) Glutamine, concentrations are in pmol gFW⁻¹. Normalized relative content of some secondary metabolites altered due to Si-treatment in clubroot-infected plants: (I) Caulilexin C; (J) Syringin; (K) Brassicanal; (L) Coniferin; (M) Indole-3-carboxaldehyde; (N) Rutalexin; (O) 4-methoxyindole-3-carboxaldehyde; (P) Brassicanate A. Error bars denote standard error of mean of three biological replicates, statistical significance ($p < 0.05$, “**”) tested using Student’s *t*-test, compared between PC and respective Si-treatment at each time point, treatments PC (Si0.0)–0.0 g Si (control), Si0.5–0.5 g Si, and Si1.0–1.0 g Si in 100 g soil-mix, inoculated with clubroot pathogen.

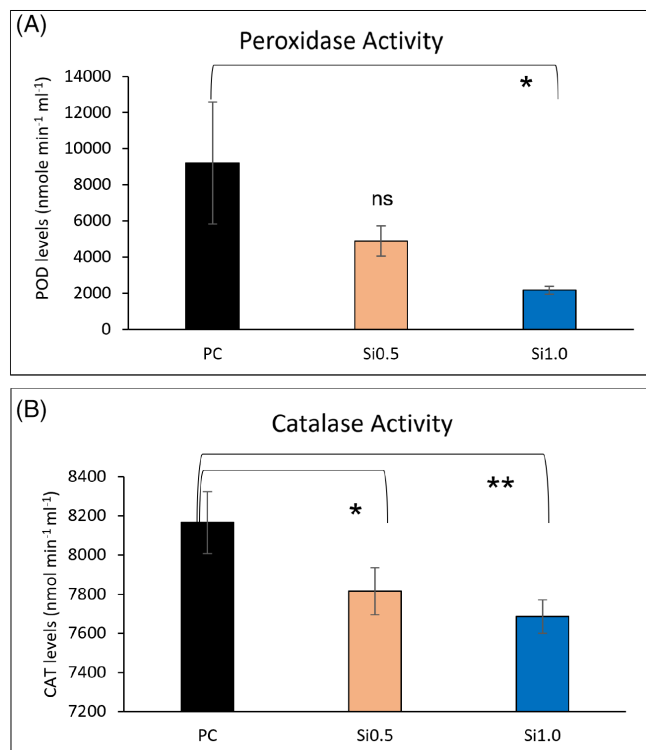


FIGURE 7 Antioxidant enzyme activity in the root samples of control (PC) and Si-treated plants at 21 days post-infection (dpi): (A) Peroxidase and (B) Catalase, measured in nmol min⁻¹ mL⁻¹. Error bars denote standard error of mean of three biological replicates, and statistical significance for Si-treated samples was calculated in comparison to PC using Student's *t*-test, denoted by the bar with “*” ($p < 0.1$) and “**” ($p < 0.05$), treatments PC (Si0.0)—0.0 g Si (control), Si0.5—0.5 g Si, and Si1.0—1.0 g Si in 100 g soil-mix, inoculated with clubroot pathogen.

several DEGs and metabolites associated with defence responses, phytohormone-mediated signal transduction, nitrogen metabolism, as well as the biosynthesis of secondary metabolites (Figure 8). Many of these altered processes were previously implicated in clubroot resistance in canola (Adhikary, Kisiala, et al., 2022a; Galindo-González et al., 2020; Summanwar et al., 2021). Moreover, some of these processes were reportedly modulated in response to Si application in other pathosystems (Feng et al., 2021; Rasoolizadeh et al., 2018). In subsequent sections, these processes are discussed in detail within the context of Si-induced protection against clubroot disease.

4.1 | Role of Si in modulating defence responses against *P. brassicae*

Plant defence hormones such as SA, JA, and ET play important roles in regulating plant responses to biotic stress. SA mediates local and systemic resistance to biotrophic/hemibiotrophic pathogens, including *P. brassicae*, leading to hypersensitivity and cell death (Bürger & Chory, 2019). During SA-mediated signalling, SA binds to the non-

expressor of PR1 (*NPR1*), which acts as a transcriptional activator for the stimulation of other defence-related genes (Wu et al., 2012). Ji et al. (2021) showed increased endogenous SA levels and upregulation of several SA-signaling genes, such as *NPR1* and *PR1*, in the susceptible *Brassica rapa* ssp. *pekinensis* in the presence of *P. brassicae*. In our study, the endogenous levels of SA were the highest, and these levels declined following Si treatment, particularly at 14 dpi (Figure 5A, Table 2). In addition, the downregulation of *NPR1* at 14 dpi, following both Si treatments, was consistent with the reduced endogenous levels of SA detected at this time point (Figure 4B, Table 1). Interestingly, Xue et al. (2021) reported inhibition of SA signalling in the potato-*Phytophthora infestans* pathosystem following foliar application of Si. Moreover, Vivancos et al. (2015) observed that SA-related defence genes were induced in the presence of a biotrophic pathogen and concluded that SA-mediated systemic signals were not necessary to induce stress tolerance by Si. In our study, the *P. brassicae* infection resulted in higher accumulation of SA, while Si treatment decreased the endogenous levels of SA, and several DEGs were associated with SA-signaling. Our observations are, therefore, consistent with those of Vivancos et al. (2015), indicating that the mode of action of Si in ameliorating clubroot disease symptoms may not involve SA signaling. However, it cannot be discounted that other effects of Si, such as higher soil pH, reduced the efficacy of the pathogen, thereby resulting in less disease severity and a consequent reduction of SA levels (and associated transcripts).

Several studies have identified important roles for JA and ET in mediating clubroot symptoms in plants (Lemarié et al., 2015; Xu et al., 2018). For instance, Xu et al. (2018) observed an increase in endogenous JA levels due to *P. brassicae* infection in susceptible *B. napus* at 14- and 28 dpi. Lemarié et al. (2015) observed JA signalling to be strongly induced in susceptible *A. thaliana*, and the exogenous application of JA reduced clubroot symptoms. Although we have not profiled the endogenous ET levels, the presence of Si resulted in lower *P. brassicae*-induced endogenous accumulation of JA in *B. napus* with a maximum reduction at 14 dpi (Figure 5B, Table 2). We also observed the downregulation of several JAZ transcripts, which function as repressors of JA-mediated signal transduction (Figure 4B, Table 1). Thus, our observations are consistent with the fact that Si treatment reduces the effect of *P. brassicae* on *B. napus*, thereby reducing the endogenous accumulation of JA.

There is an intriguing role of Si in host-pathogen interaction associated with JA and ET signalling, which has been explored in the case of several biotrophs (Fauteux et al., 2006; Ghareeb et al., 2011; Xue et al., 2021). For instance, Ghareeb et al. (2011) identified the upregulation of several JA/ET marker genes due to pathogen inoculation in the presence of Si, which was suggested to be associated with the priming potential of Si to induce defence responses. Defensins (*PDF1.2*) are known to inhibit the growth of several phytopathogens (Stotz et al., 2009) and were found to be strongly upregulated as a result of Si application in response to *Botrytis cinera* in *Arabidopsis* (Cabot et al., 2013). The expression of *PDF1.2* is modulated by the JA-ET signalling pathway, and in our study, two *PDF1.2* transcripts were

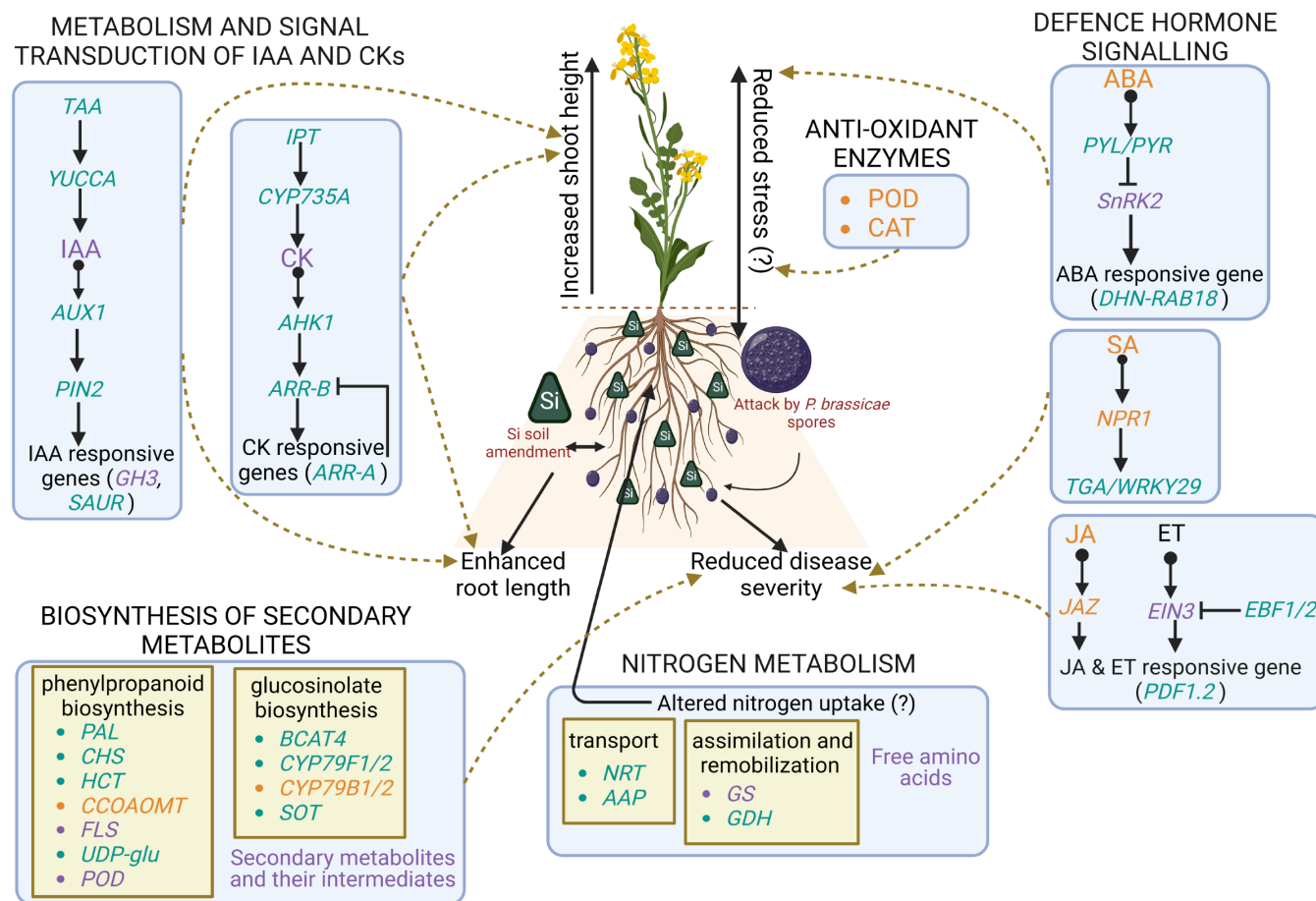


FIGURE 8 A model illustrating the role of silicon (Si) in suppressing clubroot symptoms caused by *Plasmodiophora brassicae* in *Brassica napus*. Green colored font denotes upregulation/increased accumulation, orange colored font denotes downregulation/decreased accumulation, and violet colored font shows mixed-up (increased) and down (decreased) expression due to Si amendment when compared with the control. Gene symbols have been italicized, denotes negative regulation, •- denotes interaction of a metabolite with gene. Gene names: AAP, amino acid permease; AHK1, Arabidopsis histidine kinase 1; ARR-A, two-component response regulator ARR-A family; ARR-B, two-component response regulator ARR-B family; AUX1, auxin influx carrier; BCAT4, branched chain aminotransferase 4 (methionine transaminase); CCOAOMT, caffeoyl-CoA O-methyltransferase; CHS, chalcone synthase; CYP735A, cytokinin trans-hydroxylase; CYP79B1/2, tryptophan N-monooxygenase; CYP79F1/2, homomethionine N-monooxygenase; DHN-RAB18, dehydrin response to abscisic acid 18 isoform; EBF1/2, EIN3-binding F-box protein; EIN3, ethylene-insensitive protein 3; FLS, flavonol synthase; GDH, glutamate dehydrogenase; GH3, growth hormone 3; GS, glutamine synthetase; HCT, shikimate O-hydroxycinnamoyltransferase; IPT, adenylyl isopentenyl transferase; JAZ, jasmonate ZIM domain-containing protein; NPR1, non-expressor of pathogenesis related-1; NRT, nitrate/nitrite transporter; PAL, phenylalanine ammonia-lyase; SAUR, SAUR family protein; SnRK2, serine/threonine-protein kinase SRK2; SOT, aliphatic desulfoglucosinolate sulfotransferase; TAA, L-tryptophan-pyruvate aminotransferase; UDP-glu, UDP-glucose coniferyl alcohol glucosyltransferase; WRKY29, WRKY transcription factor 29; YUCCA, indole-3-pyruvate monooxygenase. Metabolite names: ABA, abscisic acid; CAT, catalase; CK, cytokinin; ET, ethylene; IAA, auxin; JA, jasmonic acid; POD, peroxidase; SA, salicylic acid.

strongly upregulated as a result of Si treatment in *P. brassicae* infected canola root tissues (Figure 4B, Table S15). Although the JA levels were lower due to Si treatment, JA-mediated signalling has been induced as a result of Si application, which is supported by the differential expression of JA-ET-responsive genes. Taken together with past reports, the overexpression of JA- and/or ET-induced genes, for instance, *PDF1.2*, in clubroot-susceptible canola might be a viable strategy for engineering durable resistance to *P. brassicae*.

4.2 | Role of Si in ameliorating water-deficit stress in *P. brassicae* infected *B. napus*

Clubroot disease is characterized by the formation of club-shaped galls due to uncontrolled cell division around the vascular cambium (Malinowski et al., 2012). This results in water deprivation in the above-ground parts, which affects the physiology and yield potential of the plant. Increased endogenous levels of ABA in PC root samples detected in our study are indicative of stress experienced by these

plants, corresponding to gall formation (Figure 5C). Our observations are consistent with Devos et al. (2005), whereby higher endogenous ABA at 21 dpi corresponded to gall formation in *B. rapa* spp. *pekinensis* roots. Moreover, Ludwig-Müller (2009) also concluded that the host produces ABA due to water-deficit stress in response to the pathogen. Si application increased osmolyte accumulation in canola roots which improved drought tolerance and ameliorated plant growth parameters (Habibi, 2014). We observed that gall formation and progression of infection were significantly reduced in the presence of Si, particularly with Si1.0 at 21 dpi (Figure 2G–L), accompanied by consistently lower levels of ABA in the Si-treated plants (Figure 5C, Table 2). Our results suggest that the reduction in gall formation in Si-treated plants leads to lower water-deficit stress in *P. brassicae*-infected canola plants and, consequently, less endogenous ABA.

Several transcripts associated with the ABA-signaling pathway were differentially expressed due to Si treatment, and all DEGs related to *dehydrin (DHN)-response to abscisic acid RAB18* were highly upregulated following Si treatment in pathogen-challenged plants (Figure 4D, Table 1). We also previously observed an increased abundance of DHN proteins in our proteomics-based studies in a CR genotype, implicating the important role of DHNs in clubroot resistance (Adhikary, Mehta, et al., 2022b). While DHNs accumulate in plant tissues due to drought stress, they may also act as molecular chaperones and protect nucleic acids and other cellular components (Lv et al., 2018). In fact, DHN-RAB18 proteins have direct interaction with a specific membrane intrinsic aquaporin, AtPIP2B (Hernández-Sánchez et al., 2019) and, among the different families of aquaporins identified in *B. napus*, plasma membrane intrinsic proteins (PIP) were the most abundant (Sonah et al., 2017). We did not observe any differential expression of PIPs, yet we documented that DHNs were upregulated; therefore, it is reasonable to speculate that dehydrins enhance drought tolerance in Si-treated plants by altering aquaporin channel abundance and that DHN overexpression may be a viable approach to improve plant health in the presence of the pathogen.

4.3 | Role of Si in stimulating plant growth in the presence of *P. brassicae*

The development of galls caused by *P. brassicae* infection results in stunting growth, wilting, and yellowing of the above-ground parts, which culminates in premature senescence. Recently, Gou et al. (2022) reported that delayed leaf senescence in tomato due to Si treatment was accompanied by an overall increase in CK levels and an upregulation of CK biosynthesis genes under salinity stress. In our study, Si-amendment, at all concentrations, resulted in an improvement of root length in plants inoculated with *P. brassicae* (Figure 1C). Additionally, the shoot height was considerably higher in Si0.1, Si0.75, and Si1.0 (Figure 1B). This type of role of Si in improving overall plant health in response to phytopathogens is consistent with several studies (Mburu et al., 2016; Rasoolizadeh et al., 2018). Still, others have demonstrated that Si alone does not affect plant growth in the absence of either abiotic (Yin et al., 2016) or biotic (Gao et al., 2011)

stresses. Thus, it may be concluded that Si is able to improve overall plant health in the presence of biotic stress factors such as the clubroot pathogen.

As an obligate parasite, *P. brassicae* hijacks host metabolic processes through gall formation, and these hypertrophic cells become resource sinks that trap nutrients for the establishment of the pathogen during infection stages (Siemens et al., 2011). Additionally, gall formation is promoted by meristematic functions such as cell elongation and division, which results from alterations in CK and IAA homeostasis in the host plant (Malinowski et al., 2016). CKs increase the availability of essential nutrients needed for the pathogen by increasing nutrient sink strength, and hence, the roles of both CKs and IAA have been investigated in the *P. brassicae*-Brassicaceae pathosystems (Siemens et al., 2011). In our study, Si application to the pathogen-challenged plants increased the accumulation of IAA and several CKs at 7 dpi, followed by reduction at the later (14- and 21-dpi) stages (Figure 5D,E, Table 2, and Table S20). Additionally, Si treatment resulted in the upregulation of some transcripts related to IAA (e.g., *TAA*, *YUCCA*) and CK biosynthesis (e.g., *IPT*, *CYP735A*) at the later infection stages (14- and 21-dpi) (Figure 4C, Table 1). This was coincident with lower expression levels of CK degradation enzymes (CKX) (Table 1) which also leads to CK accumulation (Nguyen et al., 2021). Higher levels of CKs and IAA have been previously reported in a susceptible genotype of *B. rapa* spp. *pekinensis* when compared to a resistant genotype at later stages of infection (28 dpi) (Lan et al., 2020). In our study, increased accumulation of CKs and IAA due to Si treatment during early stages of infection (7 dpi) may be associated with stimulation of plant growth due to Si. At later stages (14- and 21-dpi), the absence of Si was associated with hypertrophy and gall formation through increased cell division, which resulted in a higher accumulation of IAA and CKs in root tissues, which is consistent with the studies mentioned above. It can, therefore, be concluded that the presence of Si reduced clubroot disease progression, which, late in the infection timeline, resulted in lower endogenous CK and IAA levels and was associated with the absence of galls.

4.4 | Role of Si in nitrogen metabolism and transport

Several studies have identified major plant health and performance improvements due to Si application through interactions with soil nutrients such as nitrogen (Xu et al., 2020). Depending on the plant species and genotype, nitrogen uptake and metabolism are affected in the presence of Si (Hodson et al., 2005). Specifically, it has been reported that Si application alters root nitrogen influx by modulating the expression of nitrate transporters (*NRT1:1* and *NRT2:1*) in both Si accumulator and non-accumulator species (Haddad et al., 2018; Wu et al., 2017). In *B. napus*, Si application delayed leaf senescence, increased plant biomass, and upregulated nitrate transporters, including *BnaNRT2.1*, under low nitrogen conditions (Haddad et al., 2018). In this study, we identified 11 DEGs belonging to different families of *NRT* (Figure 4E, Table 1), including *NRT2.1*, which were all upregulated

in the presence of Si, even under *P. brassicae* infection, which is consistent with previous studies on Si-application in *B. napus*. A recent study by Aigu et al. (2022) identified a set of genes in *B. napus* demonstrating partial resistance to clubroot under low nitrogen, and upregulation of nitrate transporters (*NRT2.1*, *NRT2.2*, and *NRT3.1*) was linked to resistance. Some of the *NRT2* genes also play an important role in defence against pathogens, and their lower expression in *A. thaliana* may contribute to susceptibility towards the plant pathogens, such as *Pseudomonas syringae* (Camañes et al., 2012) and *Erwinia amylovora* (Dechognat et al., 2012) (Aigu et al., 2022). In our study, the upregulation of *NRT2* after Si-application might have increased N-uptake by the plant, which may have improved overall plant health and development and potentially contributed to enhanced resistance against clubroot. There is, so far, no report of *NRT* genes conferring resistance to clubroot, although it is evident that they can be potential targets for further investigation.

Nitrogen uptake by plant roots alters AA biosynthesis and their remobilization from source to vegetative organs, which increases plant productivity (Tegeder & Masclaux-Daubresse, 2018). *P. brassicae* infection results in gall formation, which also affects this source-sink relationship. In our study, we determined the endogenous levels of free AAs and observed that the levels of many AAs, for example, leucine, valine, tyrosine, and methionine, were decreased at 14- and 21-dpi in the Si-treated samples (Figure 6A–G). A study by Wagner et al. (2012) reported higher accumulation of AAs in susceptible *B. napus* roots inoculated with *P. brassicae*, when compared to a resistant genotype. We also detected the highest levels of glutamine in our samples (Figure 6H), particularly at 21 dpi. Glutamine, derived from inorganic nitrogen, has been associated with SA-mediated broad-spectrum resistance, and its homeostasis may play an important role in plant-pathogen interactions (Liu et al., 2010). We can, therefore, summarize that Si presumably not only affects root nitrogen uptake by altering the expression of nitrate transporters, but it also affects primary nitrogen metabolism, including endogenous AA levels in plants infected with *P. brassicae*. These changes may manifest as a Si-mediated improvement in the plant growth parameters we evaluated.

4.5 | Role of Si in the biosynthesis of secondary metabolites in response to *P. brassicae*

Plant secondary metabolites have diverse functions, and their accumulation in response to biotic and abiotic stress enable plants to thrive in adverse environmental conditions (Isah, 2019). The role of Si in stress tolerance has also been reported through an overall increase/stimulation in the production of various secondary metabolites, including phenolics and glucosinolates, some of which possess antimicrobial properties (Ahanger et al., 2020). In addition, Si is known to reduce disease severity against plant pathogens through the upregulation of protective enzymes (such as POD, PAL), which play crucial roles in the accumulation of phenolics (e.g., lignin) and phytoalexins (Cai et al., 2008; Cherif et al., 1994). In the current study, we identified a higher proportion of DEGs related to

phenylpropanoid and glucosinolate biosynthesis that were consistently upregulated in the presence of Si at 14- and 21-dpi (Table 1, Table S6, Supporting Information File S2). Furthermore, several PODs were significantly upregulated in 14- and 21-dpi time points in Si-treated plants (Table 1, Figure 4A), and these results are consistent with the aforementioned studies investigating the role of Si during plant-pathogen interactions.

Higher expression of PODs contributes to the biosynthesis of lignin, a complex polymer formed through the oxidation of monolignols in the plant cell wall, which strengthens tissues and enhances resilience to plant pathogens (Warinowski et al., 2016). We profiled 22 secondary metabolites, including structural subunits of lignin, which are synthesized via the phenylpropanoid biosynthesis pathway, coniferyl and sinapyl alcohol glucoside, coniferin and syringin. Their endogenous levels were increased at 7 dpi, followed by a reduced accumulation at 14- and 21-dpi due to Si treatments (Figure 6J,L). Additionally, endogenous levels of POD and CAT enzymes at 21 dpi were lower in the presence of Si when compared with PC samples (Figure 7A,B).

Glucosinolates, a specific class of secondary metabolites containing nitrogen and sulfur, are characteristic of Brassicaceae and contribute to defence responses against pathogens, including *P. brassicae* (Ludwig-Müller et al., 1997; Pedras et al., 2004; Wagner et al., 2019). The majority of the glucosinolates detected in our study showed increased accumulation at 7 dpi, followed by reduced levels at later time points, concomitant with the reduction of disease severity with increasing concentration of Si (Figure 6K,M–O, Table S19). These results are consistent with Ludwig-Müller et al. (1997), whereby the total glucosinolate content in the roots of resistant genotypes of *B. campestris* spp. *pekinensis* were lower than susceptible genotypes at 14- and 20-dpi. However, in contrast to these observations, some glucosinolates and their intermediates, for example, brassicanate A, brassinin, gluconasturiin, dihydroneoascorbigen, and indole-3-acetonitrile were increased due to Si application at 21 dpi in the pathogen-challenged roots (Figure 6P, Table S19). Wagner et al. (2019) observed an accumulation of gluconasturiin in the resistant *B. napus* genotype, consistent with our results. Moreover, brassicanate A, an indolic glucosinolate, is known for its anti-fungal potential against plant pathogens, *R. solani* and *S. sclerotiorum* (Pedras et al., 2004). This is consistent with the observations of Zamani-Noor et al. (2021), where a resistant clubroot genotype exhibited increased indolic glucosinolates in the roots compared to the susceptible *B. napus* genotype. Additionally, we identified DEGs associated with glucosinolate biosynthesis, including upregulation of *BCAT4* and *CYP79F1* and downregulation of *CYP79B1/2* after Si application (Figure 4F, Table 1). Our study highlights that glucosinolate biosynthesis is altered by the presence of Si in *P. brassicae*-infected roots and, depending on the type of glucosinolate—aliphatic, aromatic, or indolic, Si application appears to differentially modulate glucosinolate levels and their associated transcripts to reduce the disease symptom. These changes in the secondary metabolites may be, among other processes, one of the mechanisms through which Si treatment ameliorates clubroot disease progression in *B. napus*.

5 | CONCLUSION

Overall, the potential of Si as a soil amendment in controlling clubroot symptoms was demonstrated, and possible mechanisms underlying Si-induced reduction of clubroot disease were revealed using an integrated “omics” approach (Figure 8). Si is an essential constituent of fertilizers that aid crop yield since it is important in stress tolerance, and its application has resulted in improvement of overall plant health. Although liming results in clubroot disease reduction, the costs associated with liming are huge. By contrast, Si is naturally available as a mineral, and some soils contain Si that plants can readily take up, depending on their needs. In addition to the potential benefits of Si treatment, our “omics” studies have resulted in the identification of several genes and metabolic pathways that may be amenable to modification using classical breeding or biotechnological approaches, including gene editing. These can contribute to the development of effective and robust strategies for the integrated management of clubroot disease, especially in the context of rapidly evolving pathotypes of *P. brassicae*.

AUTHOR CONTRIBUTIONS

Nat N. V. Kav obtained funding, supervised the project, and edited multiple versions of the manuscript. Ananya Sarkar designed, conducted the experiments and interpreted the results with input from Nat N. V. Kav and wrote the draft version of the manuscript. Dinesh Adhikary and Urmila Basu provided input into the analysis of transcriptome results and assisted with editing of draft versions of the manuscript. Habibur Rahman supplied the plant material used in this study and provided input into experimental analysis, interpretation of results and editing of the manuscript. Anna Kisiala and R. J. Neil Emery performed metabolome and phytohormone analysis and contributed to writing the relevant methods section(s) and provided input into draft versions of the entire manuscript. All authors approved the submitted version of the manuscript and declare no conflict of interest.

ACKNOWLEDGMENTS

We are grateful to Kacie Norton for her guidance in the histology work and to Swati Megha for her suggestions.

FUNDING INFORMATION

This project was supported by grant #2020F004R to Nat N. V. Kav from the Results Driven Agricultural Research (RDAR) program.

DATA AVAILABILITY STATEMENT

The clean raw RNA-sequencing data generated for this study are available under NCBI BioProject ID PRJNA905697. The metabolomics data generated have been included in the supplementary material (Tables S21 and S22) and is available at NIH Common Fund's National Metabolomics Data Repository (NMDR) website, the Metabolomics Workbench, under Study ID ST002406. The data can be assessed using project DOI: <https://doi.org/10.21228/M8M42M>.

ORCID

Nat N. V. Kav  <https://orcid.org/0000-0002-4038-4964>

REFERENCES

- Adhikary, D., Kisiala, A., Sarkar, A., Basu, U., Rahman, H., Emery, N. et al. (2022a) Early-stage responses to *Plasmodiophora brassicae* at the transcriptome and metabolome levels in clubroot resistant and susceptible oilseed *Brassica napus*. *Molecular Omics*, 18(10), 991–1014.
- Adhikary, D., Mehta, D., Uhrig, R.G., Rahman, H. & Kav, N.N.V. (2022b) A proteome-level investigation into *Plasmodiophora brassicae* resistance in *Brassica napus* canola. *Frontiers in Plant Science*, 13, 860393.
- Aebi, H. (1974) Catalase. In: Bergmeyer, H.U. (Ed.), *Methods of enzymatic analysis*. Verlag Chemie/Academic Press Inc., Weinheim/NewYork, 673–684.
- Ahanger, M.A., Bhat, J.A., Siddiqui, M.H., Rinklebe, J. & Ahmad, P. (2020) Integration of silicon and secondary metabolites in plants: a significant association in stress tolerance. *Journal of Experimental Botany*, 71(21), 6758–6774.
- Ahmed, H.U., Hwang, S.F., Strelkov, S.E., Gossen, B.D., Peng, G., Howard, R.J. et al. (2011) Assessment of bait crops to reduce inoculum of clubroot (*Plasmodiophora brassicae*) of canola. *Canadian Journal of Plant Science*, 91(3), 545–551.
- Aigu, Y., Daval, S., Gazengel, K., Marnet, N., Lariagon, C., Laperche, A. et al. (2022) Multi-omic investigation of low-nitrogen conditional resistance to clubroot reveals *Brassica napus* genes involved in nitrate assimilation. *Frontiers in Plant Science*, 13, 790563.
- Askarian, H., Akhavan, A., Manolii, V.P., Cao, T., Hwang, S.-F. & Strelkov, S. E. (2021) Virulence spectrum of single-spore and field isolates of *Plasmodiophora brassicae* able to overcome resistance in canola (*Brassica napus*). *Plant Disease*, 105(1), 43–52.
- Barr, D.J. (1992) Evolution and kingdoms of organisms from the perspective of a mycologist. *Mycologia*, 84(1), 1–11.
- Bürger, M. & Chory, J. (2019) Stressed out about hormones: how plants orchestrate immunity. *Cell Host & Microbe*, 26(2), 163–172.
- Cabot, C., Gallego, B., Martos, S., Barceló, J. & Poschenrieder, C. (2013) Signal cross talk in *Arabidopsis* exposed to cadmium, silicon, and *Botrytis cinerea*. *Planta*, 237(1), 337–349.
- Cai, K., Gao, D., Luo, S., Zeng, R., Yang, J. & Zhu, X. (2008) Physiological and cytological mechanisms of silicon-induced resistance in rice against blast disease. *Physiologia Plantarum*, 134(2), 324–333.
- Camañes, G., Victoria, P., Cerezo, M., García-Agustín, P. & Flors, V. (2012) A deletion in the nitrate high affinity transporter NRT2.1 alters metabolomic and transcriptomic responses to *Pseudomonas syringae*. *Plant Signaling & Behavior*, 7(6), 619–622.
- Cherif, M., Asselin, A. & Belanger, R.R. (1994) Defense responses induced by soluble silicon in cucumber roots infected by *Pythium spp.* *Phytopathology*, 84(3), 236–242.
- Dechorgnat, J., Patrit, O., Krapp, A., Fagard, M. & Daniel-Vedele, F. (2012) Characterization of the *Nrt2.6* gene in *Arabidopsis thaliana*: a link with plant response to biotic and abiotic stress. *PLoS One*, 7(8), e42491.
- Devos, S., Vissenberg, K., Verbelen, J.-P. & Prinsen, E. (2005) Infection of Chinese cabbage by *Plasmodiophora brassicae* leads to a stimulation of plant growth: impacts on cell wall metabolism and hormone balance. *New Phytologist*, 166(1), 241–250.
- Dixon, G.R. (2009a) The occurrence and economic impact of *Plasmodiophora brassicae* and clubroot disease. *Journal of Plant Growth Regulation*, 28(3), 194–202.
- Dixon, G.R. (2009b) *Plasmodiophora brassicae* in its environment. *Journal of Plant Growth Regulation*, 28(3), 212–228.
- Epstein, E. (2009) Silicon: its manifold roles in plants. *Annals of Applied Biology*, 155(2), 155–160.
- Fauteux, F., Chain, F., Belzile, F., Menzies, J.G. & Bélanger, R.R. (2006) The protective role of silicon in the *Arabidopsis*–powdery mildew pathosystem. *Proceedings of the National Academy of Sciences*, 103(46), 17554–17559.

- Fauteux, F., Rémus-Borel, W., Menzies, J.G. & Bélanger, R.R. (2005) Silicon and plant disease resistance against pathogenic fungi. *FEMS Microbiology Letters*, 249(1), 1–6.
- Feng, Y., Hu, Y., Fang, P., Zuo, X., Wang, J., Li, J. et al. (2021) Silicon alleviates the disease severity of sclerotinia stem rot in rapeseed. *Frontiers in Plant Science*, 12, 721436.
- Fox, N.M., Hwang, S.-F., Manolii, V.P., Turnbull, G. & Strelkov, S.E. (2022) Evaluation of lime products for clubroot (*Plasmodiophora brassicae*) management in canola (*Brassica napus*) cropping systems. *Canadian Journal of Plant Pathology*, 44(1), 21–38.
- Galindo-González, L., Manolii, V., Hwang, S.-F. & Strelkov, S.E. (2020) Response of *Brassica napus* to *Plasmodiophora brassicae* involves salicylic acid-mediated immunity: An RNA-Seq-Based study. *Frontiers in Plant Science*, 11, 1025.
- Gao, D., Cai, K., Chen, J., Luo, S., Zeng, R., Yang, J. et al. (2011) Silicon enhances photochemical efficiency and adjusts mineral nutrient absorption in *Magnaporthe oryzae* infected rice plants. *Acta Physiologiae Plantarum*, 33(3), 675–682.
- Gehrig, H.H., Winter, K., Cushman, J., Borland, A. & Taybi, T. (2000) An improved RNA isolation method for succulent plant species rich in polyphenols and polysaccharides. *Plant Molecular Biology Reporter*, 18(4), 369–376.
- Ghareeb, H., Bozsó, Z., Ott, P.G., Repenning, C., Stahl, F. & Wydra, K. (2011) Transcriptome of silicon-induced resistance against *Ralstonia solanacearum* in the silicon non-accumulator tomato implicates priming effect. *Physiological and Molecular Plant Pathology*, 75(3), 83–89.
- Gou, T., Su, Y., Han, R., Jia, J., Zhu, Y., Huo, H. et al. (2022) Silicon delays salt stress-induced senescence by increasing cytokinin synthesis in tomato. *Scientia Horticulturae*, 293, 110750.
- Habibi, G. (2014) Silicon supplementation improves drought tolerance in canola plants. *Russian Journal of Plant Physiology*, 61(6), 784–791.
- Haddad, C., Arkoun, M., Jamois, F., Schwarzenberg, A., Yvin, J.-C., Etienne, P. et al. (2018) Silicon promotes growth of *Brassica napus* L. and delays leaf senescence induced by nitrogen starvation. *Frontiers in Plant Science*, 9, 516.
- Hernández-Sánchez, I.E., Maruri-López, I., Molphe-Balch, E.P., Becerra-Flora, A., Jaimes-Miranda, F. & Jiménez-Bremont, J.F. (2019) Evidence for in vivo interactions between dehydrins and the aquaporin AtPIP2B. *Biochemical and Biophysical Research Communications*, 510(4), 545–550.
- Hodson, M., White, P.J., Mead, A. & Broadley, M.R. (2005) Phylogenetic variation in the silicon composition of plants. *Annals of Botany*, 96(6), 1027–1046.
- Hollman, K.B., Hwang, S.F., Manolii, V.P. & Strelkov, S.E. (2021) Pathotypes of *Plasmodiophora brassicae* collected from clubroot resistant canola (*Brassica napus* L.) cultivars in western Canada in 2017–2018. *Canadian Journal of Plant Pathology*, 43(4), 622–630.
- Horiuchi, S. & Hori, M. (1980) A simple greenhouse technique for obtaining high levels of clubroot [disease] incidence [of Brassica vegetables]. *Bulletin of the Chugoku National Agricultural Experiment Station Series E. Environment Division*, 17, 33–35.
- Isah, T. (2019) Stress and defense responses in plant secondary metabolites production. *Biological Research*, 52, 39.
- Jan, R., Asaf, S., Numan, M. & Kim, K.M. (2021) Plant secondary metabolite biosynthesis and transcriptional regulation in response to biotic and abiotic stress conditions. *Agronomy*, 11(5), 968.
- Ji, R., Gao, S., Bi, Q., Wang, Y., Lv, M., Ge, W. et al. (2021) The salicylic acid signaling pathway plays an important role in the resistant process of *Brassica rapa* L. ssp. *pekinensis* to *Plasmodiophora brassicae* Woronin. *Journal of Plant Growth Regulation*, 40(1), 405–422.
- Kageyama, K. & Asano, T. (2009) Life cycle of *Plasmodiophora brassicae*. *Journal of Plant Growth Regulation*, 28(3), 203–211.
- Kim, D., Paggi, J.M., Park, C., Bennett, C. & Salzberg, S.L. (2019) Graph-based genome alignment and genotyping with HISAT2 and HISAT-genotype. *Nature Biotechnology*, 37(8), 907–915.
- Kim, S.G., Kim, K.W., Park, E.W. & Choi, D. (2002) Silicon-induced cell wall fortification of rice leaves: a possible cellular mechanism of enhanced host resistance to blast. *Phytopathology*, 92(10), 1095–1103.
- Kuginuki, Y., Yoshikawa, H. & Hirai, M. (1999) Variation in virulence of *Plasmodiophora brassicae* in Japan tested with clubroot-resistant cultivars of chinese cabbage (*Brassica rapa* L. ssp. *pekinensis*). *European Journal of Plant Pathology*, 105(4), 327–332.
- Lan, M., Hu, J., Yang, H., Zhang, L., Xu, X. & He, J. (2020) Phytohormonal and metabolism analysis of *Brassica rapa* L. ssp. *pekinensis* with different resistance during *Plasmodiophora brassicae* infection. *Biocell*, 44(4), 751–767.
- Lemarié, S., Robert-Seilaniantz, A., Lariagon, C., Lemoine, J., Marnet, N., Jubault, M. et al. (2015) Both the jasmonic acid and the salicylic acid pathways contribute to resistance to the biotrophic clubroot agent *Plasmodiophora brassicae* in *Arabidopsis*. *Plant and Cell Physiology*, 56(11), 2158–2168.
- Lin, L., Allemekinders, H., Dansby, A., Campbell, L., Durance-Tod, S., Berger, A. et al. (2013) Evidence of health benefits of canola oil. *Nutrition Reviews*, 71(6), 370–385.
- Liu, G., Ji, Y., Bhuiyan, N.H., Pilot, G., Selvaraj, G., Zou, J. et al. (2010) Amino acid homeostasis modulates salicylic acid-associated redox status and defense responses in *Arabidopsis*. *The Plant Cell*, 22(11), 3845–3863.
- Liu, L., Qin, L., Zhou, Z., Hendriks, W.G., Liu, S. & Wei, Y. (2020) Refining the life cycle of *Plasmodiophora brassicae*. *Phytopathology*, 110(10), 1704–1712.
- Love, M.I., Huber, W. & Anders, S. (2014) Moderated estimation of fold change and dispersion for RNA-seq data with DESeq2. *Genome Biology*, 15(12), 1–21.
- Ludwig-Müller, J. (2009) Plant defence – what can we learn from clubroots? *Australasian Plant Pathology*, 38(4), 318–324.
- Ludwig-Müller, J., Schubert, B., Pieper, K., Ihmig, S. & Hilgenberg, W. (1997) Glucosinolate content in susceptible and resistant chinese cabbage varieties during development of clubroot disease. *Phytochemistry*, 44(3), 407–414.
- Lv, A., Su, L., Liu, X., Xing, Q., Huang, B., An, Y. et al. (2018) Characterization of dehydrin protein, CdDHN4-L and CdDHN4-S, and their differential protective roles against abiotic stress in vitro. *BMC Plant Biology*, 18(1), 1–13.
- Ma, J.F., Tamai, K., Yamaji, N., Mitani, N., Konishi, S., Katsuhara, M. et al. (2006) A silicon transporter in rice. *Nature*, 440(7084), 688–691.
- Ma, J.F., Yamaji, N., Mitani, N., Tamai, K., Konishi, S., Fujiwara, T. et al. (2007) An efflux transporter of silicon in rice. *Nature*, 448(7150), 209–212.
- Malinowski, R., Novák, O., Borhan, M.H., Spichal, L., Strnad, M. & Rolfe, S.A. (2016) The role of cytokinins in clubroot disease. *European Journal of Plant Pathology*, 145(3), 543–557.
- Malinowski, R., Smith, J.A., Fleming, A.J., Scholes, J.D. & Rolfe, S.A. (2012) Gall formation in clubroot-infected *Arabidopsis* results from an increase in existing meristematic activities of the host but is not essential for the completion of the pathogen life cycle. *The Plant Journal*, 71(2), 226–238.
- Martin, M. (2011) Cutadapt removes adapter sequences from high-throughput sequencing reads. *EMBnet.Journal*, 17(1), 10–12.
- Mburu, K., Oduor, R., Mgtutu, A. & Tripathi, L. (2016) Silicon application enhances resistance to Xanthomonas wilt disease in banana. *Plant Pathology*, 65(5), 807–818.
- Nguyen, H.N., Kambhampati, S., Kisiyala, A., Seegobin, M. & Emery, R.J.N. (2021) The soybean (*Glycine max* L.) cytokinin oxidase/dehydrogenase multigene family; Identification of natural variations for altered cytokinin content and seed yield. *Plant Direct*, 5(2), e00308.
- Pedras, M.S.C., Montaut, S. & Suchy, M. (2004) Phytoalexins from the crucifer rutabaga: structures, syntheses, biosyntheses, and antifungal activity. *The Journal of Organic Chemistry*, 69(13), 4471–4476.

- Peng, G., Pageau, D., Strelkov, S.E., Gossen, B.D., Hwang, S.-F. & Lahlali, R. (2015) A >2-year crop rotation reduces resting spores of *Plasmodiophora brassicae* in soil and the impact of clubroot on canola. *European Journal of Agronomy*, 70, 78–84.
- Perteau, M., Kim, D., Perteau, G.M., Leek, J.T. & Salzberg, S.L. (2016) Transcript-level expression analysis of RNA-seq experiments with HISAT, StringTie and Ballgown. *Nature Protocols*, 11(9), 1650–1667.
- Perteau, M., Perteau, G.M., Antonescu, C.M., Chang, T.C., Mendell, J.T. & Salzberg, S.L. (2015) StringTie enables improved reconstruction of a transcriptome from RNA-seq reads. *Nature Biotechnology*, 33(3), 290–295.
- Rahman, H., Peng, G., Yu, F., Falk, K.C., Kulkarni, M. & Selvaraj, G. (2014) Genetics and breeding for clubroot resistance in Canadian spring canola (*Brassica napus* L.). *Canadian Journal of Plant Pathology*, 36(sup1), 122–134.
- Rasoolizadeh, A., Labbé, C., Sonah, H., Deshmukh, R.K., Belzile, F., Menzies, J.G. et al. (2018) Silicon protects soybean plants against *Phytophthora sojae* by interfering with effector-receptor expression. *BMC Plant Biology*, 18(1), 1–13.
- Robinson, M.D., McCarthy, D.J. & Smyth, G.K. (2010) edgeR: a Bioconductor package for differential expression analysis of digital gene expression data. *Bioinformatics*, 26(1), 139–140.
- Schmittgen, T.D. & Livak, K.J. (2008) Analyzing real-time PCR data by the comparative CT method. *Nature Protocols*, 3(6), 1101–1108.
- Siemens, J., González, M.C., Wolf, S., Hofmann, C., Greiner, S., Du, Y. et al. (2011) Extracellular invertase is involved in the regulation of clubroot disease in *Arabidopsis thaliana*. *Molecular Plant Pathology*, 12(3), 247–262.
- Šimura, J., Antoniadi, I., Široká, J., Tarkowská, D., Strnad, M., Ljung, K. et al. (2018) Plant hormonomics: multiple phytohormone profiling by targeted metabolomics. *Plant Physiology*, 177(2), 476–489.
- Sonah, H., Deshmukh, R.K., Labbé, C. & Bélanger, R.R. (2017) Analysis of aquaporins in Brassicaceae species reveals high-level of conservation and dynamic role against biotic and abiotic stress in canola. *Scientific Reports*, 7(1), 1–17.
- Statista. (2022) Worldwide oilseed production by type 2021/22. [Accessed November 17, 2022]. Available from: <https://www.statista.com/statistics/267271/worldwide-oilseed-production-since-2008>
- Stotz, H.U., Thomson, J.G. & Wang, Y. (2009) Plant defensins. *Plant Signaling & Behavior*, 4(11), 1010–1012.
- Strelkov, S.E., Hwang, S.-F., Manolii, V.P., Cao, T. & Feindel, D. (2016) Emergence of new virulence phenotypes of *Plasmodiophora brassicae* on canola (*Brassica napus*) in Alberta, Canada. *European Journal of Plant Pathology*, 145(3), 517–529.
- Strelkov, S.E., Hwang, S.-F., Manolii, V.P., Cao, T., Fredua-Agyeman, R., Harding, M.W. et al. (2018) Virulence and pathotype classification of *Plasmodiophora brassicae* populations collected from clubroot resistant canola (*Brassica napus*) in Canada. *Canadian Journal of Plant Pathology*, 40(2), 284–298.
- Strelkov, S.E., Manolii, V.P., Cao, T., Xue, S. & Hwang, S.F. (2007) Pathotype classification of *Plasmodiophora brassicae* and its occurrence in *Brassica napus* in Alberta, Canada. *Journal of Phytopathology*, 155(11–12), 706–712.
- Strelkov, S.E., Tewari, J.P. & Smith-Degenhardt, E. (2006) Characterization of *Plasmodiophora brassicae* populations from Alberta, Canada. *Canadian Journal of Plant Pathology*, 28(3), 467–474.
- Sud, M., Fahy, E., Cotter, D., Azam, K., Vadivelu, I., Burant, C. et al. (2016) Metabolomics Workbench: An international repository for metabolomics data and metadata, metabolite standards, protocols, tutorials and training, and analysis tools. *Nucleic Acids Research*, 44(D1), D463–D470.
- Summanwar, A., Basu, U., Rahman, H. & Kav, N. (2019) Identification of lncRNAs responsive to infection by *Plasmodiophora brassicae* in clubroot-susceptible and -resistant *Brassica napus* lines carrying resistance introgressed from rutabaga. *Molecular Plant-Microbe Interactions*, 32(10), 1360–1377.
- Summanwar, A., Farid, M., Basu, U., Kav, N. & Rahman, H. (2021) Comparative transcriptome analysis of canola carrying clubroot resistance from ‘Mendel’ or Rutabaga and the development of molecular markers. *Physiological and Molecular Plant Pathology*, 114, 101640.
- Sun, F., Fan, G., Hu, Q., Zhou, Y., Guan, M., Tong, C. et al. (2017) The high-quality genome of *Brassica napus* cultivar “ZS11” reveals the introgression history in semi-winter morphotype. *The Plant Journal*, 92(3), 452–468.
- Tegeder, M. & Masclaux-Daubresse, C. (2018) Source and sink mechanisms of nitrogen transport and use. *New Phytologist*, 217(1), 35–53.
- Vivancos, J., Labbé, C., Menzies, J.G. & Bélanger, R.R. (2015) Silicon-mediated resistance of *Arabidopsis* against powdery mildew involves mechanisms other than the salicylic acid (SA)-dependent defence pathway. *Molecular Plant Pathology*, 16(6), 572–582.
- Wagner, G., Charton, S., Lariagon, C., Laperche, A., Lugan, R., Hopkins, J. et al. (2012) Metabotyping: a new approach to investigate rapeseed (*Brassica napus* L.) genetic diversity in the metabolic response to clubroot infection. *Molecular Plant-Microbe Interactions*, 25(11), 1478–1491.
- Wagner, G., Laperche, A., Lariagon, C., Marnet, N., Renault, D., Guitton, Y. et al. (2019) Resolution of quantitative resistance to clubroot into QTL-specific metabolic modules. *Journal of Experimental Botany*, 70(19), 5375–5390.
- Wallenhammar, A.C. (1996) Prevalence of *Plasmodiophora brassicae* in a spring oilseed rape growing area in central Sweden and factors influencing soil infestation levels. *Plant Pathology*, 45(4), 710–719.
- Wang, M., Gao, L., Dong, S., Sun, Y., Shen, Q. & Guo, S. (2017) Role of silicon on plant-pathogen interactions. *Frontiers in Plant Science*, 8, 701.
- Warinowski, T., Koutaniemi, S., Kärkönen, A., Sundberg, I., Toikka, M., Simola, L.K. et al. (2016) Peroxidases bound to the growing lignin polymer produce natural like extracellular lignin in a cell culture of Norway spruce. *Frontiers in Plant Science*, 7, 1523.
- Woronin, M. (1878) *Plasmodiophora brassicae*, Urheber der Kophpflanzenernie. *Jahrbucher für Wissenschaftliche Botanik*, 1, 548–574.
- Wu, X., Yu, Y., Baerson, S.R., Song, Y., Liang, G., Ding, C. et al. (2017) Interactions between nitrogen and silicon in rice and their effects on resistance toward the brown planthopper *Nilaparvata lugens*. *Frontiers in Plant Science*, 8, 28.
- Wu, Y., Zhang, D., Chu, J.Y., Boyle, P., Wang, Y., Brindle, I.D. et al. (2012) The *Arabidopsis* NPR1 protein is a receptor for the plant defense hormone salicylic acid. *Cell Reports*, 1(6), 639–647.
- Xu, D., Gao, T., Fang, X., Bu, H., Li, Q., Wang, X. et al. (2020) Silicon addition improves plant productivity and soil nutrient availability without changing the grass:legume ratio response to N fertilization. *Scientific Reports*, 10(1), 1–9.
- Xu, L., Yang, H., Ren, L., Chen, W., Liu, L., Liu, F. et al. (2018) Jasmonic acid-mediated aliphatic glucosinolate metabolism is involved in clubroot disease development in *Brassica napus* L. *Frontiers in Plant Science*, 9, 750.
- Xue, X., Geng, T., Liu, H., Yang, W., Zhong, W., Zhang, Z. et al. (2021) Foliar application of silicon enhances resistance against *Phytophthora infestans* through the ET/JA- and NPR1- dependent signaling pathways in potato. *Frontiers in Plant Science*, 12, 609870.
- Yin, L., Wang, S., Tanaka, K., Fujihara, S., Itai, A., Den, X. et al. (2016) Silicon-mediated changes in polyamines participate in silicon-induced salt tolerance in *Sorghum bicolor* L. *Plant, Cell & Environment*, 39(2), 245–258.
- Zamani-Noor, N., Hornbacher, J., Comel, C.J. & Papenbrock, J. (2021) Variation of glucosinolate contents in clubroot-resistant and -susceptible *Brassica napus* cultivars in response to virulence of *Plasmodiophora brassicae*. *Pathogens*, 10(5), 563.

Zellner, W., Tubaña, B., Rodrigues, F.A. & Datnoff, L.E. (2021) Silicon's role in plant stress reduction and why this element is not used routinely for managing plant health. *Plant Disease*, 105(8), 2033–2049.

SUPPORTING INFORMATION

Additional supporting information can be found online in the Supporting Information section at the end of this article.

How to cite this article: Sarkar, A., Kisiala, A., Adhikary, D., Basu, U., Emery, R.J.N., Rahman, H. et al. (2023) Silicon ameliorates clubroot responses in canola (*Brassica napus*): A “multi-omics”-based investigation into possible mechanisms. *Physiologia Plantarum*, 175(2), e13900. Available from: <https://doi.org/10.1111/ppl.13900>